Supplementary Material

Embodied carbon of Germany's residential stock and the emission cost of retrofitting it

[Author names withheld for double-anonymized peer review][1]

[1][Affiliation withheld for double-anonymized peer review]

October 7, 2026

List of abbreviations

AB	Apartment Building.
AM	Arithmetic Mean.
BAC	Building Age Class.
BNB	Bewertungssystem Nachhaltiges Bauen.
CV	Coefficient of Variation.
DGNB	Deutsche Gesellschaft für Nachhaltiges Bauen.
EPBD	Energy Performance of Buildings Directive.
GFA	Gross Floor Area.
GHFA	Gross Heated Floor Area.
GHG	Greenhouse Gas.
GM	Geometric Mean.
GSD	Geometric Standard Deviation.
GWP	Global Warming Potential.
IPCC	Intergovernmental Panel on Climate Change.
IQR	Interquartile Range.
LCA	Life Cycle Analysis.
LCI	Life Cycle Inventory.
LiDAR	Light Detection and Ranging.
LoD2	Level of Detail 2.
MC	Monte Carlo.
MFA	Material Flow Analysis.
MFH	Multi Family House.
NFA	Net Floor Area.
NHFA	Net Heated Floor Area.
NUTS	Nomenclature des unités territoriales statistiques.
OSM	OpenStreetMap.
PENRT	Primary Energy Non-Renewable, Total use.
PET	Primary Energy, Total use.
QNG	Qualitätssiegel Nachhaltiges Gebäude.
RegioStaR	Regional Statistical Spatial Typology for Mobility and Transport Research.
RSP	Reference Service Period.
SFH	Single Family House.
TABULA	Typology Approach for Building Stock Energy Assessment.
TH	Terraced House.
UFA	Useful Floor Area.

Supplementary Note 1 Database of building constructions

1.1 Goal, scope and system boundaries

Our database reports the life-cycle Global Warming Potential (GWP) of typical German building constructions per square meter of component, with the primary-energy indicators Primary Energy

Non-Renewable, Total use (PENRT) and Primary Energy, Total use (PET) alongside. The three environmental indicators are reported separately, so that a user can read one of them or all three. This study uses the GWP only. The intended use of the database is the assessment of the life-cycle assessment of residential building stocks with the help of three-dimensional city models, without a building-specific bill of materials. This note summarizes how it was built, but Meier-Dotzler (2023) remains the long-form documentation.

The constructions come in three families, which correspond to three things that may happen to a standing building. It can be kept as it was built. We call this family *OldBuilding*. Its thermal envelope can be improved to match a certain energetic standard, which is the *RefurbishedBuilding* family. Or it can be replaced by a new building to the Passive House standard, the *NewConstruction* family. The three families differ only in which layers they contain and which life-cycle modules are considered, as we describe in subsequent sections.

In this study, the stock account of Supplementary Note 2 uses the *OldBuilding* family, and the retrofit scenario described in Supplementary Note 4 uses the *RefurbishedBuilding* family together with *NewConstruction* windows. The reference unit of the database is one square meter of building component. Here, environmental impacts are given per square meter of Net Floor Area (NFA) (NFA according to DIN 277:2021-08 (DIN Deutsches Institut für Normung e. V., 2021)). All constructions are balanced over a standardized Reference Service Period (RSP) of 50 years.

For every construction we determined life cycle modules A1-A3 (raw-material supply, transport and manufacturing), B4 (replacement) and C3-C4 (waste processing and disposal) according to DIN EN 15978:2012-10 (DIN Deutsches Institut für Normung e. V., 2012) using the ÖKOBAUDAT dataset in version 2020-II (BMWSB, 2020; Figl et al., 2019). Module D (benefits and loads beyond the system boundary) was computed wherever the datasets supply it and is always reported separately. Standardized service lives were taken from list of service lives of building components, according to BBSR (2017), which is published for office buildings and was applied to residential construction by analogy, per material and position in the build-up. A replacement that would coincide with the end of the fifty years is not counted, so a layer with a 25-year service life is replaced once and a layer with a 50-year service life is not replaced. Modules A4 and A5 were excluded because construction-process impacts depend on the site and its transport route. No statistics exist that capture them generically at national level. Modules B1-B3 and B5 were excluded because their impacts are building- and use-specific. Modules C1 and C2 are not covered by ÖKOBAUDAT and were therefore not available.

The database covers the standard build-ups of the Cost Groups (CGs): CG 320 (foundations and substructure), CG 330 (external walls), CG 340 (internal walls), CG 350 (floors and ceilings) and CG 360 (roofs) of DIN 276:2018-12 (DIN Deutsches Institut für Normung e. V., 2018). Surface finishes such as paint and floor coverings are excluded, because they vary by project and cannot be defined generically at spatial scale. Roof overhangs and canopies are excluded and entrance doors and internal doors are measured over. Balconies and staircases are outside the boundary, because city models at Level of Detail 2 (LoD2) do not represent them.

Our database reports constructions for the following components: Pitched Roof (PRO) and Flat Roof (FRO), Top Floor Ceiling (TFL), External Wall above Ground Level (EW), Party Wall above Ground Level (SW), internal Wall (IW), Intermediate Floor Slab (FL), Basement Ceiling (CFL), Basement External Wall against Soil (CW), Party Wall in Basement (SCW), Baseplate (BP), Foundation (F) and Window (W). Several components are further split by construction method into monolithic masonry (mas), double-leaf masonry (2shelled), masonry with curtain-wall facade (cwf) and timber (wood). Windows are split by frame material into timber (wood), polyvinyl chloride (plas) and aluminum (alu). Supplementary Table 1 lists the constructions, their definitions and their mapping to the components considered in this study.

1.2 Data collection

We define eleven Building Age Classs (BACs) (Supplementary Table 2). The first nine follow the classes of the federal rules for data collection in the residential building stock (BMWi and BMI, 2020),

Supplementary Table 1: Component constructions as reported in our database and their mapping to the components considered in this study. Definitions according to Meier-Dotzler (2023). The assignment of every construction to a component is given in Supplementary Data 4 and also defined in Supplementary Note 2.1.

Component in this study	Construction recorded in the database	Definition as documented in Meier-Dotzler (2023)
Roof 1	PRO; FROmas, FROwood	Roof structure, pitched or flat, CG 361
Roof 2	TFLmas, TFLwood	Top-floor ceiling, CG 351/353/354
Wall 1	EWmas, EW2shelled, EWcwf, EWwood	External wall above ground, CG 331/332/335/336
Wall 2	CW	Basement external wall in contact with soil
Floor 1	CFLmas, CFLwood	Basement ceiling
Baseplate	BP	Base plate, CG 322/324/325 with gravel layers where reported
Foundation	F	Pad and strip foundations
Slab	FLmas, FLwood	Intermediate floor
Interior wall	IWmas, IWwood	Internal wall, CG 341–343
Window	Wwood, Wplas, Walu	Window incl. frame, glass, fittings and seals, CG 334
not used	SWmas, SW2shelled, SWcwf, SWwood; SCW	Party walls above and below ground (see Supplementary Note 2.8)

whose energy standards fix the typical layer thicknesses and insulation of each period. Later classes are split at the amendments of the German Energy Saving Ordinance of 2009 and 2013, giving BAC9 (2002-2009), BAC10 (2010-2015) and BAC11 (2016 and newer).

For the age classes up to 2001, documented constructions were taken from published catalogs and surveys, such as Zentrum für Umweltbewusstes Bauen (2009). The building profiles of Gruhler et al. (2002) contribute further constructions, such as foundations, party walls, basement walls, intermediate floors and internal walls, complemented by the building-data profiles (IÖR, n.d.). Dataholz.eu (dataholz.eu, 2021) supplies timber constructions. The typical build-ups of Thiel and Riedel (2011) and the federal data-collection rules (BMWi and BMI, 2020) supplied the period-typical U-values and layer thicknesses against which build-ups were checked. Windows were taken from the surveys of the Verband Fenster und Fassade and the Bundesverband Flachglas (Hauser et al., 2017; Verband Fenster + Fassade (VFF) and Bundesverband Flachglas (BF), n.d.). Giebeler et al. (2008) and the Typology Approach for Building Stock Energy Assessment (TABULA) typology (Loga et al., 2016) served as background on construction history and building types.

For each layer we recorded the material, its thickness, its bulk density and its thermal conductivity, taking the values from the source where given and completing them from the standard tables of DIN 4108-4:2020-11 (DIN Deutsches Institut für Normung e. V., 2020a) and DIN EN ISO 10456:2010-05 (DIN Deutsches Institut für Normung e. V., 2010) and from the history of insulation materials (Sprengard et al., 2014; Eicke-Hennig, 2017) where not. Material names were harmonized across sources, and regional information was not retained. All constructions are recorded as built, without prior refurbishment.

From 2002 onward no catalog of typical constructions exists. For these classes we developed the the building constructions as bracketing variants. The choice of load-bearing material follows the construction statistics of the Federal Statistical Office for 2003 to 2020 (Destatis, 2003–2020), and construction dimensions follow the structural design tables for masonry, reinforced concrete and timber (Bergner and Volz, 2012; Colling, 2012; Goris and Schmitz, 2012). The insulation layer follows the

Supplementary Table 2: BAC Assignment

BAC	Construction Year Interval
BAC1	< 1919
BAC2	1919–1948
BAC3	1949–1957
BAC4	1958–1968
BAC5	1969–1978
BAC6	1979–1983
BAC7	1984–1994
BAC8	1995–2001
BAC9	2002–2009
BAC10	2010–2015
BAC11	≥ 2016

required and typical U-values of the Energy Saving Ordinance in force in each age class. Waterproofing follows DIN 18531-1:2017-07 and DIN 18531-3:2017-07 for roofs and DIN 18533-1:2017-07 and DIN 18533-3:2017-07 for components in contact with soil (DIN Deutsches Institut für Normung e. V., 2017a,b,c,d).

Product data from manufacturers and trade associations complete the remaining layers, such as solid timber and glued laminated timber (Überwachungsgemeinschaft Konstruktionsvollholz e.V., 2020), cross-laminated timber (Binderholz Bausysteme GmbH, n.d.), sand-lime brick (KS-Original GmbH, 2021), clay brick (Wienerberger GmbH, 2021), aerated concrete (Xella Deutschland GmbH, n.d.), green-roof build-ups (Optigrün international AG, 2021), and hybrid timber external walls (Fischer et al., 2019).

For each component and construction method at least two variants were formed, one with the materials and construction of lowest and one of highest environmental impact at the required thermal performance. The same principle underlies the *NewConstruction* family, for which the facade shares of Asam (2017) and the baseplate detailing of the concrete industry (InformationsZentrum Beton, 2019) were additionally consulted. Data regarding windows was built from the frame and glazing types typical of each period, with timber, polyvinyl chloride and aluminum frames, on the reference window of DIN EN ISO 10077-1 (DIN Deutsches Institut für Normung e. V., 2020b).

A construction can belong to several BACs, so the number of distinct constructions is smaller than the sum over age classes. Supplementary Data 1 contains 708 distinct *OldBuilding* constructions, 676 opaque and 32 windows. Supplementary Data 2 lists 338 *RefurbishedBuilding* constructions, and Supplementary Data 3 lists 108 *NewConstruction* constructions (1,154 in total). Of the 708, 521 serve the components considered in this study. The 186 party-wall constructions are not used, because the building geometry available to us contains no shared-wall surface (see Supplementary Note 2.8). Supplementary Table 3 gives the counts by source and family. Supplementary Data 4 translates every one of the considered 521 constructions with its family, its BACs, its life-cycle GWP to the construction components of this study. For more details regarding this database, we refer to Meier-Dotzler (2023).

1.3 Life cycle modules considered in each construction family

Which life cycle modules a construction contributes to a balance depends on its role in a scenario, and not on its family alone. Supplementary Table 4 reports the rules.

The status-quo scenario records the full life cycle of every existing construction, A1-A3, B4, C3 and

Supplementary Table 3: Number (n) of constructions by source and by family. Data provided as Supplementary Data 1 to 3.

Source or family	Scope	n
Zentrum für Umweltbewusstes Bauen (2009)	Envelope components	181
Gruhler et al. (2002)	All components incl. foundations, party walls, basement walls, floors, internal walls	233
dataholz.eu (2021)	Timber constructions	21
Hauser et al. (2017)	Windows	32
OldBuilding, distinct (Supplementary Data 1)	676 opaque + 32 windows	708
of which serving the ten components of this study	Party walls excluded (see Supplementary Note 2.8)	522
of which entering the estimation described in Supplementary Note 2	PRO_1 excluded (see Supplementary Note 2.4)	521
NewConstruction (Supplementary Data 3)	Passivhaus standard, 100 opaque + 8 windows	108
RefurbishedBuilding (Supplementary Data 2)	KfW-55 shell, opaque components only	338
Total		**1,154**

Supplementary Table 4: Life-cycle modules considered for a construction according to its role in a scenario based on Meier-Dotzler (2023). *Year 50* denotes the end of the reference study period.

Role of the construction in a scenario	A1–A3	B4	C3–C4	D
Existing construction, status quo, all components	yes	yes	yes, at year 50	separate
Existing construction retained through a refurbishment	no	yes	yes, at year 50	separate
Existing construction demolished	no	no	yes, immediately	separate
Refurbishment, layer removed	no	no	yes, immediately	separate
Refurbishment, layer added	yes	yes	yes, at year 50	separate
Refurbishment, layer retained	no	yes	yes, at year 50	separate
New construction	yes	yes	yes, at year 50	separate

C4, for all components. Its product stage is a present-day equivalent. The ÖKOBAUDAT datasets describe current production, so the A1-A3 of an existing construction states what its impacts would be if it were built the same way today, and not the emissions of its historical production. Where an existing construction is retained during a refurbishment, only modules B4 and C3-C4 at year 50 contribute, because its production stage can no longer be influenced.

A refurbishment construction starts from an existing construction of the same component and age class and adds, removes or replaces layers to reach the building shell of a KfW Efficiency House 55 standard. *Efficiency House* 55 (*Effizienzhaus* 55, EH-55) is a German energy-performance standard in which a building is limited to 55% of the primary energy demand of an equivalent reference building defined in German building law. *KfW*, *Kreditanstalt für Wiederaufbau*, is the German development bank that administers the subsidy program naming the class. We chose it because it is the technical minimum requirement of the KfW for subsidized energy-efficient refurbishment, and because the insulation thicknesses it requires are constructively easier to realize than those of the Passive House standard. Layers that are removed are recorded with their C3 and C4. Layers that are added contribute A1-A3, B4 and C3-C4. Layers that remain are booked with B4 and C3-C4 only. While focusing on the energetic retrofit, only the thermal envelope is refurbished (see also Supplementary Note 4). Internal walls, intermediate floors, foundations and party walls are not refurbished. Also, windows are not

refurbished, but replaced instead: an old window is recorded with its C3 and C4, and its replacement is a *NewConstruction* window booked with A1-A3, B4 and C3-C4.

The *NewConstruction* family reproduces constructions aligned with the Passive House standard (Passive House Institute, 2023). This study uses the *NewConstruction* family only for the replacement windows of the retrofit scenario.

For each component construction and BAC across all building construction families our database reports a life cycle module split (A1-A3, B4, and C3-C4) of two constructions: a representative minimum and a representative maximum. These minima and maxima are selected by a normalization over the three environmental performance indicators GWP, PENRT, and PET. For each construction the A1-C4 total of GWP, of PENRT and of PET is calculated, a negative total is set to zero, each total is divided by the largest value of its indicator in the pool, and the three ratios are summed to a score between 0 and 3. The constructions with the lowest and the highest score form the minimum and maxmimum pair. The score combines the indicators because a construction can have the lowest GWP of its pool and, at the same time, a high total primary-energy demand.

1.4 What the database does not represent

The product stage of an existing construction is a present-day equivalent. Constructions are recorded as built, and refurbishments carried out before the reference period are not represented (Cischinsky and Diefenbach, 2016). Surface finishes, doors, balconies and staircases are outside the boundary, so module B4 is a lower bound (Schneider-Marin et al., 2019). The construction catalog sources carry no information on how common each construction is, so no statistical weight can be attached to any construction on a spatial level. The thermal utilization of wood at end of life is the standard scenario in ÖKOBAUDAT. Hence, a cascading use of recovered wood would change the ranking of timber constructions (Höglmeier et al., 2013) and their consideration in the minimum and maximum impact derivation. Modules A4, A5, B1-B3, B5, C1 and C2 are not covered.

Supplementary Note 2 Embodied GWP Calculation Methodology

2.1 Notation

Before presenting the calculation procedure, we establish a transparent notation:

- Buildings: $i \in \{1, \ldots, N\}$ denotes an individual building.
- Structural components: $c \in \mathcal{C} = \{\text{Roof1}, \text{Roof2}, \text{Wall1}, \text{Wall2}, \text{Floor1}, \text{Baseplate}, \text{Foundation}, \text{Slab}, \text{InteriorWall}, \text{Window}\}$. Roof1 denotes roof construction exposed to external air, Roof2 is the top-floor ceiling bordering unheated spaces, Wall1 indicates an external wall facing outdoor air, Wall2 is a wall in contact with soil, and Floor1 is the floor above an unheated cellar. Baseplate is the ground-bearing slab and Foundation the strip and pad footings beneath it. Slabs are all vertically separating structures not classified as Roof2, Floor1, or Baseplate.
- Building size class: $s \in \{\text{SFH}, \text{TH}, \text{MFH}, \text{AB}\}$.
- Building age class: $b \in \{\text{BAC1}, \ldots, \text{BAC11}\}$, assigned by construction year (see Supplementary Table 2).
- Construction family: $\sigma \in \{\text{OldBuilding}, \text{RefurbishedBuilding}, \text{NewConstruction}\}$.
- Life cycle module: $m \in \mathcal{M} = \{\text{A1–A3}, \text{B4}, \text{C3–C4}\}$, the three module groups of DIN EN 15978:2012-10 (DIN Deutsches Institut für Normung e. V., 2012) covered by the assessment. A1–A3 is product-stage manufacturing, B4 is component replacement over the reference study period, and C3–C4 is end-of-life waste processing and disposal. A superscript m denotes the part of a GWP quantity attributable to module group m, so that $\text{gwp}_j^{\text{A-C}} = \sum_{m \in \mathcal{M}} \text{gwp}_j^m$ for any construction j.
- Representative construction set: $\mathcal{R}_{c,k}$ is the set of constructions for which we report module-resolved GWP for component c under class key k, namely the minimum- and maximum-impact construction of each construction type serving that component (see Supplementary Equation (3)).
- Module bounds: $\text{gwp}_{c,k}^{m,\min}$ and $\text{gwp}_{c,k}^{m,\max}$ ($\text{kg CO}_2\text{e/m}^2$) are the module-$m$ intensities of the minimum- and maximum-impact representative construction of component c under class k.
- Spatial unit: $\mathcal{G} \subseteq \{1, \ldots, N\}$ is any set of buildings over which results are aggregated, from a single 1 km grid cell to the national stock $\mathcal{G} = \{1, \ldots, N\}$.
- Building class key: $k = (b, \sigma)$, the tuple of age class and construction family used to look up construction intensities.
- Construction set: $\mathcal{A}_{c,k}$ is the set of constructions applicable to component c and building class k.
- **Notation convention**: uppercase GWP denotes *building-level aggregates* and lowercase gwp denotes *component-level intensities* ($\text{kg CO}_2\text{e/m}^2$).
- Construction count: $n_{c,k} = |\{j \in \mathcal{A}_{c,k} : \text{gwp}_j > 0\}|$, the number of positive gwp constructions.
- Component area: $A_{c,i}$ (m^2) is the area of structural component c for building i.
- Conditioned living area: $A_{l,i}$ (m^2) of building i comes from ETHOS.BUILDA (Dabrock et al., 2024b) and equals $A_N/1.3$, where A_N is the usable floor space.
- TABULA wall ratio: $r_{s,b,\ell}$ ($\text{m}^2\,\text{m}^{-2}$), the empirical exterior wall-to-living area ratio from TABULA (Loga et al., 2012) for size class s, construction period group b, and A_l size bin ℓ.

Supplementary Table 5: Data sources used in this study.

Source	Dataset content	Usage
Dabrock et al. (2024b)	ETHOS.BUILDA: German residential building stock incl. characteristics such as footprint area, height, living area, construction year, size class, refurbishment state, and roof shape	Building-level geometry for component area estimation and GWP calculation
Meier-Dotzler (2023)	Structural assembly GWP intensities ($\mathrm{kg\,CO_2e/m^2}$) clustered by BAC and refurbishment state.	Individual reference intensities for each building class
Loga et al. (2012, 2016)	TABULA: Typology-derived building characteristics differentiated by BAC and refurbishment state.	Fallback mechanism when ETHOS.BUILDA lacks input

- Other size-class specific ratios: ρ_s is the interior-wall-to-exterior-wall ratio, and ω_s is the window-to-wall ratio. FTBP_b is the foundation-to-base-plate ratio and is BAC-specific. All ratios based on Meier-Dotzler (2023).
- Reference service life: $T = 50$ years, used to annualize the building-level embodied GWP.
- NFA $A_{\mathrm{NFA},i}$ ($\mathrm{m^2}$) is equal to the conditioned floor area $A_{l,i}$ of building i.

2.2 Overview

Embodied GWP is calculated at the individual building level using structural component areas derived from building footprint and height data (Dabrock et al., 2024b), combined with material-specific construction gwp values from our database (see Supplementary Data 1 to 3). According to DIN EN 15978:2012-10 (DIN Deutsches Institut für Normung e. V., 2012), we capture life-cycle modules A1-A3 (product stage), B4 (replacement), and C3-C4 (waste processing and disposal) via the $\mathrm{GWP_{A\text{-}C}}$ indicator. We summarize the main datasets and their usage in Supplementary Table 5.

ETHOS.BUILDA derives building geometry through two pipelines selected by federal state. Ten states use a Level-of-Detail-2 (LoD2) pipeline built from the official three-dimensional building cadaster and airborne LiDAR. T he remaining six, namely Baden-Württemberg, Bremen, Mecklenburg-Vorpommern, Rhineland-Palatinate, Saarland and Schleswig-Holstein, draw footprints from OpenStreetMap and obtain building heights from a machine-learning model (Dabrock et al., 2024a).

2.3 Building Classification

In order to define age class b, each building is assigned to one of 11 BACs based on its construction year (see Supplementary Table 2), following TABULA (Loga et al., 2016).

Building size class s comes directly from Dabrock et al. (2024b) and distinguishes Single Family Houses (SFHs), Terraced Houses (THs), Multi Family Houses (MFHs), and Apartment Buildings (ABs). Size classes s are aligned with the TABULA schema.

The resulting sample is summarized in Supplementary Table 6. The stock is dominated by SFHs, followed by MFHs. Together the two classes account for over 91% of the residential stock. Median NFA ranges from $110\,\mathrm{m^2}$ in THs to $1{,}573\,\mathrm{m^2}$ in ABs. Median construction year lies between 1958 (ABs) and 1964 (THs), and most of the stock falls in age classes BAC3–BAC5. Across all size classes, nearly 62%

Supplementary Table 6: Descriptive statistics of the ETHOS.BUILDA data sample, stratified by building size class

			Building characteristics: median (IQR)				Refurbishment
s[a]	n [Mio.]	%	Height [m]	Footprint [m^2]	NFA [m^2]	Constr. Year	NotRef/Ref[b][%]
TH	1.57	8.1	9.1 (7.8–10.1)	67 (59–80)	110 (90–138)	1964 (1954–1974)	39.3/60.7
SFH	14.93	76.9	8.6 (7.6–9.6)	111 (84–148)	160 (115–227)	1962 (1952–1972)	38.0/62.0
MFH	2.84	14.6	11.8 (9.2–14.3)	152 (106–210)	341 (189–577)	1960 (1950–1970)	38.5/61.5
AB	0.08	0.4	21.2 (17.3–23.8)	313 (228–482)	1,573 (1,003–2,685)	1958 (1904–1971)	40.7/59.3
Germany	19.42						38.2/61.8

[a] Size classes s: SFH = Single-family House, TH = Terraced house, MFH = Multi-family House, AB = Apartment Building.
[b] NotRef = not refurbished (ETHOS refurbishment state 1); Ref = refurbished (ETHOS refurbishment states 2 or 3)

of buildings carry a refurbished label. Because that label is assigned probabilistically and identifies no individual building, it does not enter our estimation (Supplementary Note 2.6).

Each ETHOS.BUILDA record further carries a refurbishment state. Dabrock et al. (2025) follow the TABULA schema and distinguish three states, labeled *existing* (ETHOS.BUILDA refurbishment state 1), *usual* (ETHOS.BUILDA refurbishment state 2), and *advanced* (ETHOS.BUILDA refurbishment state 3), which correspond to the categories *not refurbished*, *partially refurbished*, and *fully refurbished* reported at federal state level by Metzger et al. (2019). This attribute is not predicted per building. Dabrock et al. (2025) state that no reliable source with building-level data for the assignment of refurbishment states could be identified, and assign the attribute probabilistically so that the resulting distribution reproduces the federal state shares in Metzger et al. (2019). Within a federal state, the refurbishment attribute is therefore independent of construction year, size class, and geometry, and it identifies no individual building. Across all size classes, nearly 62% of buildings carry a refurbished label. Because that label is assigned probabilistically and identifies no individual building, it does not enter our estimation (Supplementary Note 2.6).

We organize constructions into three families. *OldBuilding* constructions describe age-typical construction as built(*Status Quo*), which spans BAC1 to BAC11. *RefurbishedBuilding* constructions describe a prospective energetic renovation of those constructions to the KfW Efficiency House 55 standard (*Refurbishment*). *Efficiency House* 55 (*Effizienzhaus* 55, EH-55) is a German energy-performance standard in which a building is limited to 55% of the primary energy demand of an equivalent reference building defined in German building law. *KfW*, *Kreditanstalt für Wiederaufbau*, is the German development bank that administers the subsidy programme naming the class. *NewConstruction* constructions describe replacement construction to Passivhaus standard (*Deconstruction and Newbuild*). Only the *OldBuilding* family is descriptive of an existing stock.

Three consequences follow for the present assessment. First, the ETHOS.BUILDA refurbishment attribute cannot select which buildings receive which construction family, because it locates no individual building. Second, neither dataset records the depth of a refurbishment that has already taken place. Third, the *RefurbishedBuilding* pools are constructed as an impact range instead of a census of documented renovations, and admit no central estimate (Supplementary Note 2.4). We therefore fix $\sigma = \text{OldBuilding}$ for every building, so that the building class key reduces to the age class:

$$k_i = (b_i, \text{OldBuilding}), \qquad b_i \in \{\text{BAC1}, \ldots, \text{BAC11}\} \tag{1}$$

Hence a building constructed in 1969 is assigned $k = (\text{BAC5}, \text{OldBuilding})$ irrespective of its labeled refurbishment state. The resulting indicator describes the German residential stock *as originally built*, and every building-level estimate rests only on BAC b and size class s. Because Metzger et al. (2019) report that a majority of the stock has undergone some refurbishment, the standing stock

embodies more than our estimation. Neither the *RefurbishedBuilding* nor the *NewConstruction* family is evaluated. Both describe interventions, not standing constructions, and pricing the refurbishment increment requires constructions these data do not contain, as Supplementary Note 2.4 sets out. They belong to a forward scenario analysis.

2.4 Ecological Performance of Structural Building Components

Construction-level gwp intensities $\mathrm{gwp}_{c,k}$ are derived based on the description in Supplementary Note 1. We present an overview of the number of constructions within each construction family and component, with summary statistics of their ecological performance, in Supplementary Table 7. The table reports all three families, including the two that our estimation does not use, because they document the database in full and support future scenario evaluation.

For example, the dataset documents 157 individual constructions for the building component *Wall1* in the family *OldBuilding*, while we only have 12 constructions for the same component in the family *NewConstruction*. Assemblies are organized by family σ and BAC b. Multiple constructions may apply to the same component c across multiple BACs b, but never across multiple families. For this reason, we generate building class key $k = (b, \sigma)$, which enables pooling constructions into $\mathcal{A}_{c,k}$ within building components. Another reason for this approach is that we are effectively unable to locate individual constructions used in the building stock on the individual building level.

Because our estimation fixes $\sigma = \mathrm{OldBuilding}$, the pools it draws on are $\mathcal{A}_{c,(b,\mathrm{OldBuilding})}$ across all ten components and all eleven BACs. Of these 110 pools, 107 are populated and the smallest holds a single construction (*Wall2* in BAC2). The three empty pools are *Foundation* in BAC9 to BAC11, where a raft foundation is assumed and the component carries no area (Supplementary Equation (16)), so no construction is required. Construction counts rise from BAC1 to BAC11 in step with construction practice where the BAC11 pools describe modern as-built construction.

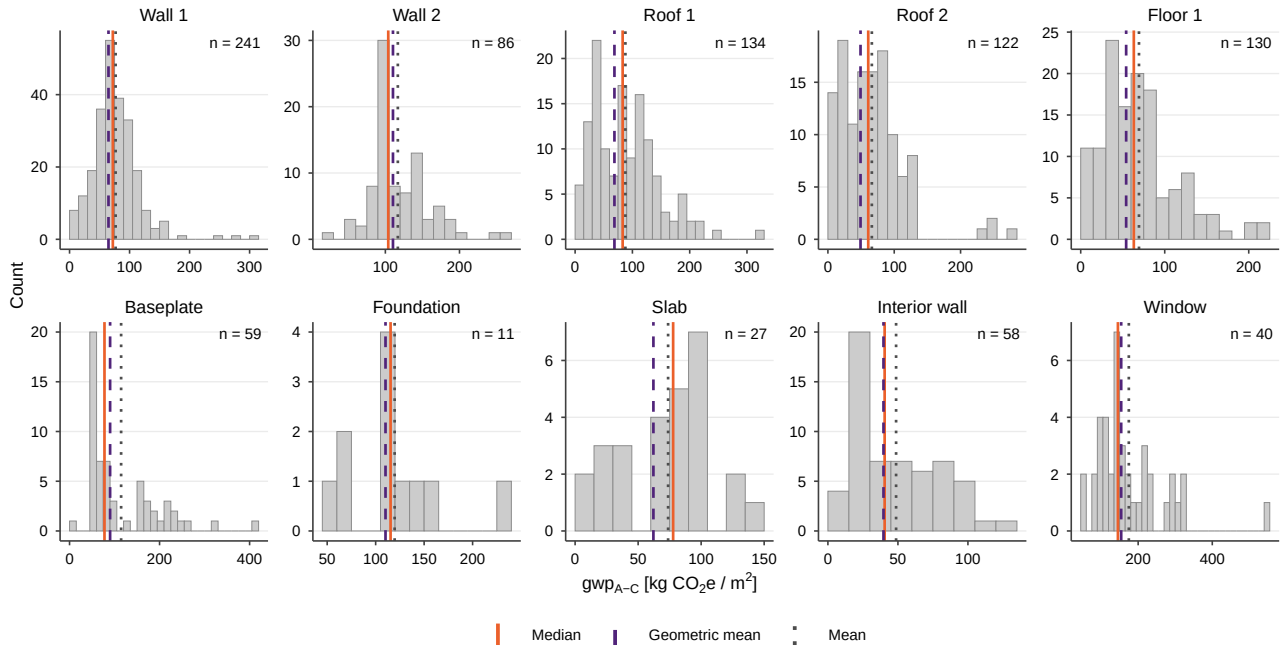
As Supplementary Table 7 shows, the dataset provides no *RefurbishedBuilding* constructions for components *Slab*, *InteriorWall*, and *Window*, and these pools are empty at every BAC. Renovation constructions are only developed for the thermal envelope. We treat interior walls and slabs as irrelevant to energetic improvement and assume that windows are replaced in full instead of refurbished.

The *RefurbishedBuilding* pools that do exist are not documented renovations. For each component and BAC, we identify the two *OldBuilding* constructions with the normalized minimum and maximum impacts, and derives from each the renovation variants causing the lowest and the highest impacts. The stated aim is that at least four renovation variants per component and BAC describe the bandwidth of possible impacts, and the count rises with each construction method distinguished within a component. The pool is therefore a range by design. A geometric mean over it locates the center of a set of bounds and estimates no central tendency, so we read the *RefurbishedBuilding* family only through its minimum and maximum. The *OldBuilding* pools carry no such construction and are a distribution of the documented catalog, which is what Supplementary Equation (2) requires.

Qin and Suh (2017) documented that Life Cycle Inventory (LCI) data is skewed and follows a lognormal distribution. This phenomenon was later confirmed by Pomponi and Moncaster (2018). A histogram of structural assemblies clustered by components c confirms this tendency, as Supplementary Fig. 1 shows. The orange solid line shows the median, the purple dashed line the geometric mean and the dotted black line the arithmetic mean. With the exception of *Slab*, all other components have greater mean than median values. Long right tails are especially present in components *Wall1, Wall2, Roof1, Floor1, Baseplate, Window*.

Hence, we aggregate the warming potential intensities using the geometric mean:

$$\overline{\mathrm{gwp}}_{c,k} = \exp\left(\frac{1}{n_{c,k}} \sum_{\substack{j \in \mathcal{A}_{c,k} \\ \mathrm{gwp}_j > 0}} \ln\left(\mathrm{gwp}_j\right)\right) \tag{2}$$



Supplementary Figure 1: **Distribution of construction-level embodied carbon intensity, by building component.** Documented constructions, pooled by structural component c and reported as the A–C total per square meter of construction. Each panel is one of the ten components, and n is the number of documented constructions in that component's pool. Vertical lines mark the median (orange, solid), the geometric mean (purple, dashed) and the arithmetic mean (black, dotted). Every component except *Slab* has an arithmetic mean above its median, and the long right tails visible in *Wall 1*, *Wall 2*, *Roof 1*, *Floor 1*, *Baseplate* and *Window* motivate the geometric-mean estimator of Supplementary Equation (2).

where $\mathcal{A}_{c,k}$ is the set of constructions belonging to class k and component c, and $n_{c,k} = |\{j \in \mathcal{A}_{c,k} : \text{gwp}_j > 0\}|$. Note that constructions with $\text{gwp}_j = 0$ are excluded from both the summation and the count $n_{c,k}$, since $\ln(0)$ is undefined. However, this removes only one construction for roofs ("PRO1" in class key k = (BAC1, OldBuilding)) from the data. PRO1 carries gwp = -74.58 kg $\text{CO}_2\text{e}/\text{m}^2$ (see Supplementary Data 1). All other construction entries are positive.

We resolve construction gwp into the three module groups $m \in \mathcal{M}$, so that a reported total is $\text{gwp}_j^{\text{A-C}} = \text{gwp}_j^{\text{A1-A3}} + \text{gwp}_j^{\text{B4}} + \text{gwp}_j^{\text{C3-C4}}$. This resolution is not published for every construction of a pool. Following the normalization procedure described in Supplementary Note 1.3 and Supplementary Equation (3), we identify for each component and BAC the constructions causing the minimum and the maximum environmental impact, and report the module-resolved gwp of those two constructions only. A module decomposition of the pooled geometric mean would require gwp_j^m for all $j \in \mathcal{A}_{c,k}$ and is therefore not computable from the published data.

Two properties of the estimator would obstruct such a decomposition even if the full module vectors were available. Module groups are not additive under the geometric mean, since $\sum_{m\in\mathcal{M}} \text{GM}(\text{gwp}^m) \neq \text{GM}(\text{gwp}^{\text{A-C}})$ unless the module vectors are proportional across the pool. Group A1–A3 is also negative for every construction whose materials sequester more carbon during production than their disposal releases, so a geometric mean would be undefined across part of the pool, and excluding those constructions would remove the lowest-impact options from the A1–A3 pool alone.

We therefore carry module information as a range instead of a decomposition of the point estimate. The geometric-mean point estimate (Supplementary Equation (2)) remains our estimate of the A–C total, and the module range is reported alongside it. Let $\mathcal{R}_{c,k}$ denote the set of representative constructions for which module-resolved $\text{gwp}^{\text{A-C}}$ is reported for component c under class key k. Where

several construction types serve the same component, $\mathcal{R}_{c,k}$ holds the reported minimum and maximum of each type and the selection ranges over all of them. The bounding constructions follow from the A–C total:

$$j_{c,k}^{\min} = \arg\min_{j \in \mathcal{R}_{c,k}} \mathrm{gwp}_j^{\text{A-C}}, \qquad j_{c,k}^{\max} = \arg\max_{j \in \mathcal{R}_{c,k}} \mathrm{gwp}_j^{\text{A-C}} \tag{3}$$

and the module range of the component is read from those two constructions:

$$\mathrm{gwp}_{c,k}^{m,\min} = \mathrm{gwp}_{j_{c,k}^{\min}}^{m}, \qquad \mathrm{gwp}_{c,k}^{m,\max} = \mathrm{gwp}_{j_{c,k}^{\max}}^{m}, \qquad m \in \mathcal{M} \tag{4}$$

where group C3–C4 is formed within each construction as $\mathrm{gwp}_j^{\text{C3-C4}} = \mathrm{gwp}_j^{\text{C3}} + \mathrm{gwp}_j^{\text{C4}}$. Each bound is one construction rather than a per-module extremum, so its module groups sum to its own total:

$$\sum_{m \in \mathcal{M}} \mathrm{gwp}_{c,k}^{m,\min} = \mathrm{gwp}_{j_{c,k}^{\min}}^{\text{A-C}}, \qquad \sum_{m \in \mathcal{M}} \mathrm{gwp}_{c,k}^{m,\max} = \mathrm{gwp}_{j_{c,k}^{\max}}^{\text{A-C}} \tag{5}$$

so the decomposition is exactly additive within each bound and at every level of aggregation. An individual module group may run in the opposite direction to the total, since the minimum-impact construction of a component is not the minimum in every group. The base plate from BAC9 onward illustrates this, where the minimum-impact construction carries the higher A1–A3 intensity and the lower C3–C4 intensity of the two bounds.

Two properties of $\mathcal{R}_{c,k}$ qualify the range. First, we identify the bounding constructions by normalizing $\mathrm{gwp}^{\text{A-C}}$, PENRT, and PET jointly and by setting negative GWP values to zero before ranking, so the pair brackets a representative (not a maximum) range and the lower bound does not reach the carbon-storing constructions that the normalization sets aside. Supplementary Equation (3) ranks the reported constructions by gwp alone, which is a different criterion from the one that selected them. Second, the resulting bounds do not coincide with the extremes of the sampled pool $\mathcal{A}_{c,k}$ and are not a subset of it. It is therefore reported as the representative range applied to the stock, and it is distinct from the construction-choice bounds of the sampling design in Supplementary Note 3.

2.5 Component Area Estimation

Conditioned Living Area The ETHOS.BUILDA dataset provides a conditioned living area variable $A_{l,i}$, derived from the heated building volume V_i as:

$$A_{l,i} = \frac{0.32 \cdot V_i}{1.3}, \qquad V_i = A_{f,i} \cdot \max(h_i - r_i,\ 3.5\,\mathrm{m}) \tag{6}$$

where $A_{f,i}$ is the footprint area, h_i is the ridge-line building height, and r_i is an area-weighted roof height correction (Dabrock et al., 2024b). The factor $0.32\,\mathrm{m}^{-1}$ converts volume to A_N following Loga et al. (2012), and the divisor 1.3 converts A_N to conditioned living area following Meier-Dotzler (2023).

Above-Ground Exterior Wall Area (Wall1) The above-ground exterior wall area is estimated by applying empirical facade ratios from Loga et al. (2012) to $A_{l,i}$:

$$A_{\mathrm{Wall1},i} = r_{s,b,\ell} \cdot A_{l,i} \tag{7}$$

where $r_{s,b,\ell}$ is the exterior wall-to-living area ratio for size class s, construction period group b, and A_l size bin ℓ. Supplementary Table 8 distinguishes two typological groups (SFH/TH with ≤ 2 dwelling units, and MFH/AB with ≥ 3 dwelling units), three construction period groups, and three size bins ℓ. A size correction is applied for buildings with $A_{l,i} > 400\,\mathrm{m}^2$, as Loga et al. (2012) document declining area-to-volume and exterior wall-to-living area ratios for larger buildings. Note that their sample is skewed towards SFH and small MFH with large MFH and AB being underrepresented. The resulting lookup table is:

The $A_l > 400\,\mathrm{m}^2$ values for MFH are derived by applying a size discount factor of 0.8 following Loga et al. (2012). AB ratios are extrapolated from the MFHs gradient, as ABs are not documented in Loga et al. (2012).

Interior Walls and Windows Size class specific window-to-wall ω_s and interior-wall-to-exterior-wall ρ_s ratios are applied to $A_{\mathrm{Wall1},i}$ following Meier-Dotzler (2023):

$$A_{\mathrm{Window},i} = \omega_s \cdot A_{\mathrm{Wall1},i}, \qquad A_{\mathrm{InteriorWall},i} = \rho_s \cdot A_{\mathrm{Wall1},i} \tag{8}$$

where $\omega_s = \begin{cases} 0.12 & s \in \{\mathrm{SFH}, \mathrm{TH}\} \\ 0.15 & s \in \{\mathrm{MFH}, \mathrm{AB}\} \end{cases} \qquad \rho_s = \begin{cases} 0.54 & s \in \{\mathrm{SFH}, \mathrm{TH}\} \\ 1.34 & s \in \{\mathrm{MFH}, \mathrm{AB}\} \end{cases}$

Below-Ground Exterior Wall Area (Wall2) The below-ground exterior wall *Wall2* has no empirical TABULA basis and we were unable to find empirically justified perimeter-to-footprint relationships in the literature for below-ground building envelopes in Germany. *Wall2* is therefore approximated as:

$$A_{\mathrm{Wall2},i} = 4\sqrt{A_{f,i}} \cdot h_{\mathrm{cellar}}, \qquad h_{\mathrm{cellar}} = 2\,\mathrm{m} \tag{9}$$

This assumes a square building footprint, for which the perimeter equals $4\sqrt{A_{f,i}}$. Interior walls below ground are assigned for MFH and AB, using the ratio $\rho_s = 1.34$. SFH and TH are assumed to have no below-ground interior walls.

Roof, Floor and Slab Areas The ETHOS.BUILDA dataset provides multiple different roof shapes. Because exact roof areas cannot be computed from architecturally complex shapes without detailed geometric data, all non-flat roofs are modeled as pitched roofs with a uniform pitch angle. Roof pitch in Germany exhibits a clear north-south gradient: steep roofs with pitches around 60°and short eaves are common in northern Germany, whereas shallower pitches (typically around 30°) with large eaves predominate in the south (Baunetz Wissen, 2024). For simplification, a single representative angle of $\alpha = 7\pi/36$ (equal to 35°) is adopted, broadly consistent with the pan-German modal pitch class. Schlemminger et al. (2024) show that, on average, more than 60% of buildings have pitched roofs with angles between 28 and 48 degrees. Hence, roof height contribution and component areas are:

$$h_{\mathrm{roof}} = \begin{cases} 0 & \text{flat or unknown roof} \\ \dfrac{\sqrt{A_{f,i}}}{2} \tan\alpha & \text{pitched roof} \end{cases} \tag{10}$$

$$h_{\mathrm{wall}} = h_i - h_{\mathrm{roof}} \tag{11}$$

$$A_{\mathrm{Roof1}} = \begin{cases} A_{f,i} & \text{flat or unknown roof} \\ A_{f,i}/\cos\alpha & \text{pitched roof} \end{cases} \tag{12}$$

A building's number of storeys and internal slabs are then derived from wall heights h_{wall}:

$$n_{\mathrm{storeys}} = \max\left(\mathrm{round}\left(\frac{h_{\mathrm{wall}}}{h_{\mathrm{storey}}}\right), 1\right), \qquad h_{\mathrm{storey}} = 2.5\,\mathrm{m} \tag{13}$$

$$n_{\mathrm{slabs}} = \max(n_{\mathrm{storeys}} - 1,\ 0) \tag{14}$$

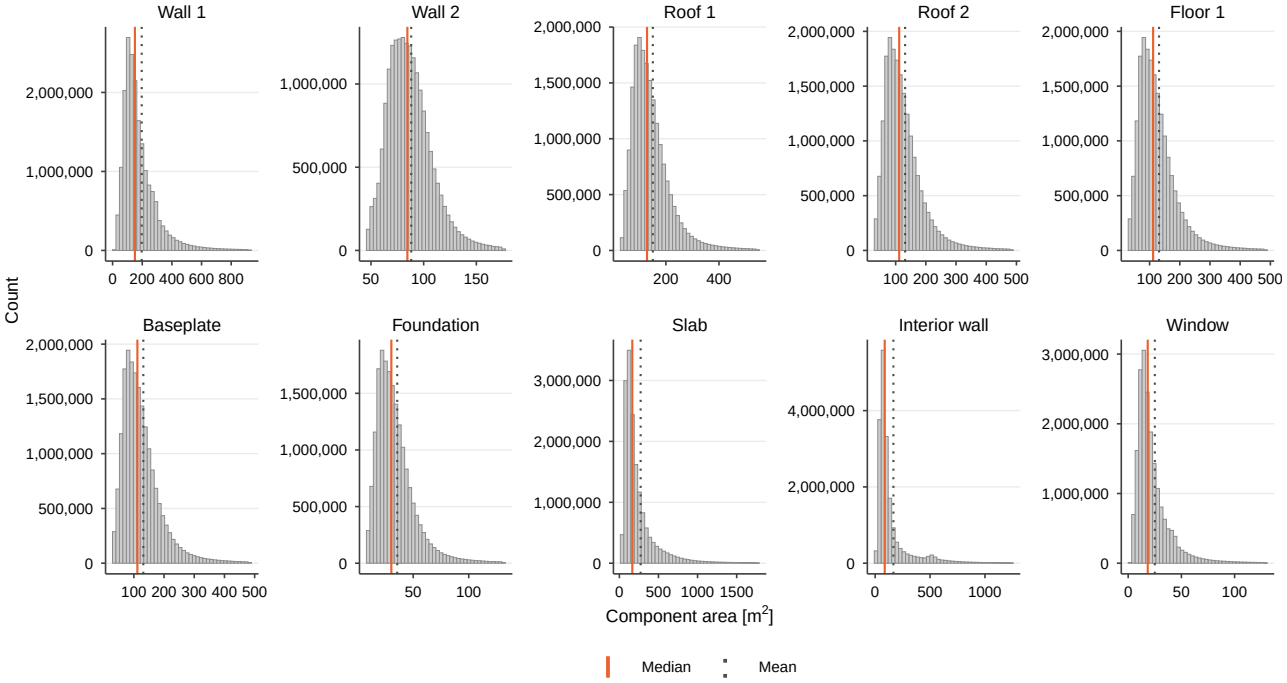
Finally, we treat the ground-bearing slab and the footings beneath it as distinct constructions. The base plate covers the building footprint, and the foundation area follows from it through the foundation-to-base-plate ratio FTBP_b:

$$A_{\text{Baseplate},i} = A_{f,i} \qquad A_{\text{Foundation},i} = \text{FTBP}_{b_i} \cdot A_{f,i} \tag{15}$$

$$\text{FTBP}_b = \begin{cases} 0.27 & b \in \{\text{BAC1}, \ldots, \text{BAC8}\} \\ 0 & b \in \{\text{BAC9}, \text{BAC10}, \text{BAC11}\} \end{cases} \tag{16}$$

Meier-Dotzler (2023) derives FTBP = 0.27 as the mean across 18 building records, ranging from 0.59 for MFHs in BAC1 to zero for MFHs in BAC6 and BAC7. From BAC9 onward we assume a raft foundation, in which the base plate itself transfers the load and its thickness already accounts for the material mass that separate footings would otherwise add, so no foundation is modeled and FTBP_b is set to zero.

We summarize all area definitions and formulas in Supplementary Table 9. Supplementary Fig. 2 shows the healthy variation of building component areas in the dataset. The orange solid line indicates the median, whereas the black dotted line shows the arithmetic mean. Because of the large relative presence of SFHs, the distributions are heavily skewed, with median and mean dominating the lower end.



Supplementary Figure 2: **Distribution of estimated component surface areas across the standing stock.** Component areas derived from building-specific geometry for every building in the sample, one panel per structural component, in square meters. Vertical lines mark the median (orange, solid) and the arithmetic mean (black, dotted). All ten distributions are right-skewed, because single-family houses dominate the stock by count and concentrate each distribution at the low end.

2.6 GWP Calculation

The total GWP per building is the sum of ten structural component contributions:

$$\text{GWP}_i = \sum_{c \in \mathcal{C}} A_{c,i} \cdot \overline{\text{gwp}}_{c,k_i}, \quad k_i = (b_i, \text{OldBuilding}) \tag{17}$$

where $\mathcal{C}$ is the set of structural components c, $A_{c,i}$ is the area of component c for building i, and $\overline{\text{gwp}}_{c,k_i}$ is the geometric-mean construction intensity for component c under building class key k_i.

The lifetime-normalized GWP indicator is

$$\mathrm{GWP}_{\mathrm{m^2a},i} = \frac{\mathrm{GWP}_i}{A_{\mathrm{NFA},i} \cdot T} \tag{18}$$

where $A_{\mathrm{NFA},i}$ is the net floor area in m^2 and $T = 50$ years is the assumed reference study period. GWP_i is given in $\mathrm{kg\,CO_2e}$ and $\mathrm{GWP}_{\mathrm{m^2a},i}$ in $\mathrm{kg\,CO_2e/(m^2{\cdot}a)}$.

2.7 Module decomposition

Applying Supplementary Equation (4) to the same component areas bounds the same building by life cycle module:

$$\mathrm{GWP}_i^{m,\min} = \sum_{c \in \mathcal{C}} A_{c,i} \cdot \mathrm{gwp}_{c,k_i}^{m,\min}, \qquad \mathrm{GWP}_i^{m,\max} = \sum_{c \in \mathcal{C}} A_{c,i} \cdot \mathrm{gwp}_{c,k_i}^{m,\max} \tag{19}$$

where $\mathrm{GWP}_i^{m,\min}$ and $\mathrm{GWP}_i^{m,\max}$ are the parts of building i's embodied GWP attributable to module group m under the minimum- and maximum-impact constructions of each of its components. By Supplementary Equation (5) the three groups sum to the corresponding bound of the building total, so the range partitions each bound without residual.

The partition separates emissions already released from those still to be incurred, resolving the latter into two flows that differ in when they arise. Group A1–A3 is fixed at the time of construction and is *sunk* for the standing stock. Group B4 is *recurring* over the service life through component replacement. Group C3–C4 is *contingent* on an end-of-life decision not yet taken:

$$\begin{aligned} \mathrm{GWP}_i^{\mathrm{sunk},\min} &= \mathrm{GWP}_i^{\text{A1-A3},\min}, & \mathrm{GWP}_i^{\mathrm{sunk},\max} &= \mathrm{GWP}_i^{\text{A1-A3},\max} \\ \mathrm{GWP}_i^{\mathrm{recurring},\min} &= \mathrm{GWP}_i^{\mathrm{B4},\min}, & \mathrm{GWP}_i^{\mathrm{recurring},\max} &= \mathrm{GWP}_i^{\mathrm{B4},\max} \\ \mathrm{GWP}_i^{\mathrm{contingent},\min} &= \mathrm{GWP}_i^{\text{C3-C4},\min}, & \mathrm{GWP}_i^{\mathrm{contingent},\max} &= \mathrm{GWP}_i^{\text{C3-C4},\max} \end{aligned} \tag{20}$$

Because Supplementary Equation (19) is evaluated for every building from its own component areas and age class, the range aggregates to any spatial unit $\mathcal{G}$ by the same operation as Supplementary Equation (18):

$$\mathrm{GWP}_{\mathrm{m^2a},\mathcal{G}}^{m,\min} = \frac{\sum_{i \in \mathcal{G}} \mathrm{GWP}_i^{m,\min}}{T \cdot \sum_{i \in \mathcal{G}} A_{\mathrm{NFA},i}}, \qquad \mathrm{GWP}_{\mathrm{m^2a},\mathcal{G}}^{m,\max} = \frac{\sum_{i \in \mathcal{G}} \mathrm{GWP}_i^{m,\max}}{T \cdot \sum_{i \in \mathcal{G}} A_{\mathrm{NFA},i}} \tag{21}$$

where $\mathcal{G}$ is any set of buildings, from a single 1 km grid cell to a Nomenclature des unités territoriales statistiques (NUTS)-3 district, a federal state, or the national stock $\mathcal{G} = \{1, \ldots, N\}$. Both quantities carry the units and the normalization of Supplementary Equation (18), so the range and the point estimate are directly comparable at every scale. Aggregation is weighted by NFA, so a unit's range reflects the floor area its buildings carry, not their count.

2.8 Summary of Key Assumptions

1. All buildings are assumed to have a cellar with a height of $h_{\mathrm{cellar}} = 2\,\mathrm{m}$.
2. Cellars and roofs are not conditioned (unheated), consistent with the TABULA framework.
3. Below-ground exterior wall area *Wall2* is approximated as $4\sqrt{A_{f,i}} \cdot h_{\mathrm{cellar}}$, assuming a square footprint whose perimeter equals $4\sqrt{A_{f,i}}$.
4. Roof pitch is uniformly set to $\alpha = 35°$ for all non-flat roofs and unknown roof shapes are treated as flat.
5. Storey height is fixed at $h_{\mathrm{storey}} = 2.5\,\mathrm{m}$, and building height follows the ridge-line definition of Dabrock et al. 2025.

6. The base plate covers the full building footprint. The foundation area is the FTBP_b fraction of it (Supplementary Equation (16)) and zero from BAC9 onward where a raft foundation is assumed (Meier-Dotzler, 2023).

7. TH buildings are treated as fully detached (no shared-wall deduction).

8. AB wall area ratios are extrapolated from the MFH area-to-volume gradient and carry no direct TABULA empirical basis.

9. In line with DIN EN 15978 (DIN Deutsches Institut für Normung e. V., 2012), the RSP is set to 50 years for the annualization of GWP.

10. Our estimation fixes the construction family, so $k_i = (b_i, \mathrm{OldBuilding})$.

11. The *RefurbishedBuilding* pools are an impact range by design and carry a different module boundary from the *OldBuilding* family (see Supplementary Table 4).

12. Module-resolved gwp is published only for the minimum- and maximum-impact construction of each component and BAC, so the module partition is reported as a range (Supplementary Equations (3) and (4)) and not as a decomposition of the geometric-mean point estimate. The bounding constructions were selected on GWP, PENRT, and PET jointly, so the reported span is representative and not maximal.

Supplementary Table 7: Construction gwp intensities ($gwp_{A\text{-}C}$) disaggregated by family and structural component. Full documentation of all constructions is given in Supplementary Data 1 to 3.

			$gwp_{A\text{-}C}$ [kg CO_2e/m^2]				
Family[a]	Component[b]	n[c]	min	median	geom. mean	mean	max
OB	Roof1	63	8.4	39.0	40.9	53.3	187.4
OB	Roof2	62	4.9	34.0	32.7	44.8	119.5
OB	Wall1	157	0.8	75.0	61.7	74.3	162.2
OB	Wall2	42	26.0	110.0	107.3	115.1	190.3
OB	Floor1	64	5.4	71.3	56.3	66.0	150.5
OB	Baseplate	23	2.7	78.1	81.3	114.2	419.2
OB	Foundation	11	59.3	115.4	110.2	119.6	234.7
OB	Slab	22	11.8	78.5	66.7	76.3	145.1
OB	InteriorWall	46	6.7	41.8	40.6	49.4	128.0
OB	Window	32	45.5	141.6	148.0	171.2	552.2
RB	Roof1	62	53.2	112.7	113.0	121.4	324.1
RB	Roof2	54	12.6	78.8	75.4	89.7	275.5
RB	Wall1	72	27.8	68.4	68.1	77.6	304.3
RB	Wall2	28	86.3	93.2	99.5	100.4	136.0
RB	Floor1	60	8.8	51.3	49.9	70.2	218.3
RB	Baseplate	32	48.9	68.6	90.5	107.7	318.6
RB	Foundation	0	—[d]	—	—	—	—
RB	Slab	0	—	—	—	—	—
RB	InteriorWall	0	—	—	—	—	—
RB	Window	0	—	—	—	—	—
NC	Roof1	10	22.5	90.2	77.1	93.4	193.8
NC	Roof2	6	41.3	76.9	71.6	76.5	129.4
NC	Wall1	12	25.7	102.4	94.8	104.8	182.3
NC	Wall2	16	63.9	144.4	141.9	150.2	256.8
NC	Floor1	6	31.2	89.5	79.8	96.5	172.6
NC	Baseplate	4	83.8	171.9	156.6	172.4	262.0
NC	Foundation	0	—	—	—	—	—
NC	Slab	5	11.8	43.4	45.4	62.6	127.2
NC	InteriorWall	12	6.7	37.9	36.3	46.1	90.4
NC	Window	8	139.5	162.9	181.7	189.3	318.8

[a] OB = Old Building, RB = Refurbished Building, NC = New Construction.
[b] Roof1 is a roof element exposed to external air. Roof2 is the top-floor ceiling bordering unheated spaces such as a cold attic. Wall1 indicates an external wall facing outdoor air. Wall2 is a wall in contact with soil. Floor1 is the ceiling above an unheated cellar. Baseplate is the ground-bearing slab covering the footprint, and Foundation the strip or pad footings beneath it.
[c] n is the count of assemblies mapped to each (construction family, component) pool; a single physical construction may be mapped to multiple components, so n summed across components can exceed the unique-assembly total. Alignment of constructions with components C is reported in Supplementary Data 4.
[d] — indicates an empty pool.

Supplementary Table 8: Wall area ratios $r_{s,b,\ell}$ (exterior wall-to-living area, $\mathrm{m}^2\,\mathrm{m}^{-2}$)

Typology	Period	$A_l \leq 175\,\mathrm{m}^2$	$175 < A_l \leq 400\,\mathrm{m}^2$	$A_l > 400\,\mathrm{m}^2$
SFH / TH	≤ 1978	1.04	1.04	–
SFH / TH	1979–1994	0.94	0.94	–
SFH / TH	≥ 1995	0.97	0.97	–
MFH	≤ 1978	0.76	0.76	0.64
MFH	1979–1994	0.72	0.72	0.61
MFH	≥ 1995	0.74	0.74	0.62
AB	all periods	–	0.69	0.55

Supplementary Table 9: Structural component area definitions

Component	Identifier	Derivation
Exposed roof construction	Roof1	Supplementary Equation (12)
Top-floor ceiling	Roof2	—
External wall above ground	Wall1	Supplementary Equation (7)
External wall below ground	Wall2	Supplementary Equation (9)
Floor above unheated cellar	Floor1	—
Foundation / Floor on ground	Foundation / Baseplate	Supplementary Equation (15) / Supplementary Equation (16)
Intermediate slab	Slab	Supplementary Equation (14)
Interior wall above ground	InteriorWall	Supplementary Equation (8)
Window	Window	Supplementary Equation (8)

Supplementary Note 3 Monte Carlo Sensitivity Analysis

3.1 Motivation

The GWP calculation (Supplementary Equation (17), Supplementary Note 2) uses a single geometric-mean construction intensity $\overline{\mathrm{gwp}}_{c,k}$ for every building in class $k = (b, \text{OldBuilding})$. In practice, the actual assembly installed in any given building is unknown, and two structurally distinct uncertainties are conflated in the point-estimate formulation. Construction-choice uncertainty asks which of the $n_{c,k}$ eligible constructions was used, and is a building-level quantity. Estimator bias arises from the geometric mean itself, since the arithmetic mean of the eligible pool is by construction higher than its geometric mean for any non-degenerate, strictly positive pool, and is a class-level quantity.

This section documents the procedure used to quantify both. Construction-choice uncertainty is quantified by an empirical bootstrap Monte Carlo (MC) at the archetype level, with archetypes stratified by federal state so that cross-state differences in building geometry and stock composition (Supplementary Table 10) are not blurred by a single national archetype. Estimator bias is quantified analytically in closed form from the pool itself, without sampling, as $\Delta_{\alpha}^{\mathrm{arith}}$ defined below. Uncertainty in geometric characteristics $A_{f,i}$, h_i, $A_{l,i}$ is documented in Dabrock et al. (2025) and is not propagated here.

Supplementary Table 10: Archetype context by federal state: building type share, stock-weighted mean footprint area, and NUTS-3 sampling

	Type share [%]				Mean footprint [m^2]				NUTS-3	
Federal state	SFH	TH	MFH	AB	SFH	TH	MFH	AB	Available	Sampled[a]
Baden-Wuertt.	74.8	7.8	17.3	0.1	138	80	169	387	44	10
Bavaria	82.1	7.3	10.0	0.7	130	79	205	329	96	10
Berlin	55.1	8.3	26.0	10.6	107	73	305	456	1	1
Brandenburg	88.8	3.5	7.6	0.1	113	84	271	508	18	10
Bremen	31.7	37.1	30.9	0.4	136	71	164	399	2	2
Hamburg	55.5	17.5	26.2	0.8	114	82	292	674	1	1
Hesse	78.6	8.6	12.6	0.2	101	74	159	384	26	10
Lower Saxony	85.8	5.8	8.4	0.1	135	78	207	464	45	10
Meckl.-Vorp.	78.9	5.3	15.4	0.5	134	88	226	570	8	8
N. Rh.-Westph.	65.8	12.3	21.8	0.1	118	77	169	417	53	10
Rhineland-Pal.	83.5	5.6	10.8	0.1	142	88	174	403	36	10
Saarland	82.3	7.3	10.3	0.1	135	91	156	375	6	6
Saxony	75.9	3.2	20.5	0.4	126	84	200	298	13	10
Saxony-Anhalt	81.5	5.1	13.1	0.2	132	101	183	256	14	10
Schleswig-H.	77.9	9.4	12.6	0.1	147	81	202	447	15	10
Thuringia	84.5	4.0	11.4	0.1	92	75	181	554	22	10
Total									**400**	**128**

[a] NUTS-3 regions sampled per federal state (up to 10 each) to derive archetype geometry; 128 sampled of 400 available.

Three sampling modes are used. *Uniform* is the empirical bootstrap. *Min* and *max* are deterministic bounds that select the minimum or maximum intensity from each pool, providing lower and upper scenario bounds under fully correlated extreme-choice construction substitution.

3.2 Notation

All notation follows Supplementary Note 2 unless otherwise noted. Additional symbols introduced here are

- Archetype $\alpha = (\text{fed}, b, s)$, a unique combination of federal state (*fed*), age class b, and size class s. The construction family is fixed to *OldBuilding* throughout and is therefore not part of the archetype.
- Archetype geometry $\tilde{A}_{f,\alpha}$, $\tilde{h}_\alpha$, $\tilde{A}_{l,\alpha}$, $\tilde{A}_{\mathrm{NFA},\alpha}$ for the median footprint area, height, conditioned living area, and NFA across buildings of archetype α. Roof shape $\tilde{\kappa}_\alpha$ is the modal category (pitched if $\geq 50\%$ of buildings in α are non-flat, else flat).
- Arithmetic-mean construction intensity $\overline{\mathrm{gwp}}^{\mathrm{arith}}_{c,k} = \frac{1}{n_{c,k}} \sum_{j \in \mathcal{A}_{c,k}} \mathrm{gwp}_j$, over the same pool and index j as Supplementary Equation (2).
- Sampling mode index $r \in \{\text{uniform, min, max}\}$.
- MC draw index $d \in \{1, \ldots, D\}$, where $D = 1{,}000$. The symbol m is reserved for life cycle module groups in Supplementary Note 2.
- Mode-specific construction intensity $\widehat{gwp}^{(d,r)}_{c,k}$ selected for component c, class k, draw d, mode r.
- Mode-specific archetype $\widehat{\mathrm{GWP}}^{(d,r)}_{\alpha}$ in $\mathrm{kg\,CO_2e/(m^2{\cdot}a)}$ for archetype α in draw d under mode r, annualized over the reference study period T as in Supplementary Equation (18).
- Federal states $\text{fed} \in \mathcal{F}$, $|\mathcal{F}| = 16$.
- Class key of archetype α: $k(\alpha) = (b_\alpha, \text{OldBuilding})$, following our estimation (Supplementary Note 2.3).

3.3 Procedure

The procedure consists of four steps.

1. *Build the construction pool.* The construction pool is constructed identically to Supplementary Note 2. Only constructions with $\mathrm{gwp}_{A\text{-}C} > 0$ are retained. Only the *OldBuilding* pools are retained, and these are pre-split into a list indexed by the age class b. Of the 110 component-by-age-class pools, 107 are populated (Supplementary Note 2). The three empty pools are the *Foundation* pools of BAC9 to BAC11, which carry no area under Supplementary Equation (16) and are never queried, so no substitution is required.

2. *Derive archetype geometry per federal state.* Within each federal state $\text{fed} \in \mathcal{F}$, up to 10 NUTS-3 regions are sampled uniformly at random (Supplementary Table 10). Archetypes $\alpha = (\text{fed}, b, s)$ span a grid of $16 \times 11 \times 4 = 704$ cells, of which 672 are populated in the sample. These draw on 6,456,059 buildings from the 128 sampled NUTS-3 regions, a subset of the full 19.42-million-building stock. Each populated archetype is formed by grouping buildings and computing

$$\tilde{A}_{f,\alpha} = \mathrm{median}_{i \in \alpha}(A_{f,i}) \tag{22}$$

$$\tilde{h}_\alpha = \mathrm{median}_{i \in \alpha}(h_i) \tag{23}$$

$$\tilde{A}_{l,\alpha} = \mathrm{median}_{i \in \alpha}(A_{l,i}) \tag{24}$$

$$\tilde{A}_{\mathrm{NFA},\alpha} = \mathrm{median}_{i \in \alpha}(A_{\mathrm{NFA},i}) \tag{25}$$

$$\tilde{\kappa}_\alpha = \begin{cases} \text{pitched} & \text{if } \bar{p}_\alpha \geq 0.5 \\ \text{flat} & \text{otherwise} \end{cases} \tag{26}$$

   where $\bar{p}_\alpha$ is the proportion of buildings in α with a non-flat roof shape.

3. *Monte Carlo sampling.* For each archetype α, each mode r, and each draw d

   (a) Component areas $\{A_{c,\alpha}\}_{c\in\mathcal{C}}$ are computed once from archetype geometry using the area formulas in Supplementary Note 2.5, and fixed across all D draws.

   (b) For each component $c \in \mathcal{C}$, one construction intensity is selected from the eligible pool $\mathcal{A}_{c,k(\alpha)}$ according to mode r

$$\widehat{gwp}_{c,k}^{(d,r)} = \begin{cases} \text{draw with replacement from } \mathcal{A}_{c,k(\alpha)}, & r = \text{uniform} \\ \min\big(\mathcal{A}_{c,k(\alpha)}\big), & r = \min \\ \max\big(\mathcal{A}_{c,k(\alpha)}\big), & r = \max \end{cases} \tag{27}$$

   (c) The annualized archetype GWP per unit NFA for draw d and mode r is

$$\widehat{\mathrm{GWP}}_{\alpha}^{(d,r)} = \frac{1}{\tilde{A}_{\mathrm{NFA},\alpha}\cdot T}\sum_{c\in\mathcal{C}} A_{c,\alpha}\cdot \widehat{gwp}_{c,k}^{(d,r)} \tag{28}$$

   For $r =$ uniform, this is repeated $D = 1{,}000$ times per archetype. For $r = \min$ and $r = \max$, $\widehat{\mathrm{GWP}}_{\alpha}^{(d,r)}$ is degenerate across d by construction.

4. *Output statistics.* For each archetype α, two point estimates and three uncertainty statistics are reported. The point estimates are the geometric-mean archetype GWP

$$\overline{\mathrm{GWP}}_{\alpha}^{\mathrm{geom}} = \frac{1}{\tilde{A}_{\mathrm{NFA},\alpha}\cdot T}\sum_{c\in\mathcal{C}} A_{c,\alpha}\cdot \overline{\mathrm{gwp}}_{c,k(\alpha)} \tag{29}$$

   and the arithmetic-mean archetype GWP

$$\overline{\mathrm{GWP}}_{\alpha}^{\mathrm{arith}} = \frac{1}{\tilde{A}_{\mathrm{NFA},\alpha}\cdot T}\sum_{c\in\mathcal{C}} A_{c,\alpha}\cdot \overline{\mathrm{gwp}}_{c,k(\alpha)}^{\mathrm{arith}} \tag{30}$$

   computed from arithmetic-mean construction intensities applied to the same archetype geometry. Supplementary Equation (30) is the uniform-prior expectation, equal in the limit to the mean of the MC output under uniform sampling, and requires no sampling to compute. All three archetype quantities are annualized over $T = 50$ years and are reported in $\mathrm{kg\,CO_2e/(m^2{\cdot}a)}$, matching Supplementary Equation (18) so that archetype and building-level estimates are directly comparable.

   The three uncertainty statistics are the one-directional bias

$$\Delta_{\alpha}^{\mathrm{arith}} = \frac{\overline{\mathrm{GWP}}_{\alpha}^{\mathrm{arith}} - \overline{\mathrm{GWP}}_{\alpha}^{\mathrm{geom}}}{\overline{\mathrm{GWP}}_{\alpha}^{\mathrm{geom}}} \tag{31}$$

   of the geometric-mean estimator against the arithmetic-mean point estimate, the geometric standard deviation

$$\mathrm{GSD}_{\alpha} = \exp\left(\mathrm{SD}\left(\ln \widehat{\mathrm{GWP}}_{\alpha}^{(d,\mathrm{uniform})}\right)\right) \tag{32}$$

   of the MC output as a multiplicative dispersion measure on the natural scale of strictly-positive right-skewed data, and the empirical 90% interval

$$\left[\hat{Q}_{0.05}^{\mathrm{uniform}}(\alpha),\ \hat{Q}_{0.95}^{\mathrm{uniform}}(\alpha)\right] \tag{33}$$

   where $\hat{Q}_{p}^{\mathrm{uniform}}(\alpha)$ denotes the p-quantile of $\left\{\widehat{\mathrm{GWP}}_{\alpha}^{(d,\mathrm{uniform})}\right\}_{d=1}^{D}$. The *min* and *max* modes are deterministic bound outputs carrying no variation, reported as lower and upper scenario bounds, not probability statements.

3.4 Analytical basis for the bias

The sign of $\Delta_\alpha^{\text{arith}}$ is determined by the inequality between the arithmetic and geometric means. For any pool of $n_{c,k} \geq 2$ strictly positive construction intensities,

$$\overline{\text{gwp}}_{c,k}^{\text{geom}} = \exp\left(\frac{1}{n_{c,k}} \sum_{j \in \mathcal{A}_{c,k}} \ln \text{gwp}_j\right) \leq \overline{\text{gwp}}_{c,k}^{\text{arith}} = \frac{1}{n_{c,k}} \sum_{j \in \mathcal{A}_{c,k}} \text{gwp}_j \tag{34}$$

with equality only when all intensities are identical. Because Supplementary Equation (28) and Supplementary Equation (30) share the same geometry $\{A_{c,\alpha}\}$ and net floor area $\tilde{A}_{\text{NFA},\alpha}$, the inequality carries through to the archetype level. $\Delta_\alpha^{\text{arith}}$ is therefore non-negative in every archetype α, and strictly positive whenever any component pool contains more than one distinct intensity.

The construction pools are approximately lognormal, a structure documented by Qin and Suh (2017), confirmed by Pomponi and Moncaster (2018) and visible in the construction LCI histograms (Supplementary Fig. 1). For such pools the per-component bias admits the second-order approximation

$$\frac{\overline{\text{gwp}}_{c,k}^{\text{arith}} - \overline{\text{gwp}}_{c,k}^{\text{geom}}}{\overline{\text{gwp}}_{c,k}^{\text{geom}}} \approx \frac{\sigma_{\ln,\,c,k}^2}{2} \tag{35}$$

where $\sigma_{\ln,\,c,k}^2$ is the variance of ln(gwp) within cell (c,k). The archetype-level $\Delta_\alpha^{\text{arith}}$ is a GWP-weighted average of the per-component biases across $c \in \mathcal{C}$, and therefore grows with the within-pool dispersion of the dominant components in each archetype.

The bias is interpretable as a quantified uncertainty margin on the geometric-mean point estimate under the uniform prior. It is not a probability statement about the true embodied GWP of any specific building, since the uniform prior is itself a modeling assumption (Supplementary Note 3.5).

3.5 Assumptions

1. Constructions are sampled independently within each class $k = (b, \text{OldBuilding})$ in the *uniform* mode (Supplementary Equation (27)). The age-class stratification absorbs era-level correlation across components, so a pre-1919 wall construction cannot draw alongside a post-2015 slab construction in the same pool. Residual within-class correlation (e.g. material-family coherence, sub-vintage matching) cannot be estimated because our construction database records gwp intensities without material, regional, or construction-tradition metadata. The *min* and *max* modes bound the effect of this residual correlation, since any monotone correlation structure across components is bracketed by the deterministic *min*/*max* bounds.

2. Each construction within $\mathcal{A}_{c,k}$ is sampled with equal probability $1/n_{c,k}$. This is an uninformative prior that assumes no knowledge of which construction types dominate the German stock.

3. The *min* and *max* modes are deterministic stress-test bounds under extreme component-wise choices. They define lower and upper bounds for scenario comparison and do not provide probabilistic confidence intervals.

4. We do not differentiate construction intensities by federal state, so the same pool $\mathcal{A}_{c,k}$ enters the bootstrap for all 16 federal states. Cross-state differences in $\widehat{\text{GWP}}_\alpha^{(d,r)}$ reflect differences in archetype geometry only, not differences in regional material prevalence.

5. Component areas $\{A_{c,\alpha}\}$ are derived from median building geometry within each state and held constant across all D draws. Uncertainty in ETHOS.BUILDA's geometric attributes ($A_{f,i}$, h_i, $A_{l,i}$) is not propagated here, isolating construction-choice uncertainty from geometric uncertainty.

6. Of the 107 populated (c, b) pools, one contains a single eligible construction (*Wall2* in BAC2) and four contain two (*Slab* in BAC1 and BAC2, *InteriorWall* in BAC2, *Floor1* in BAC8). In those cells the component returns the same value across all D draws and contributes no variance to GSD_α and no bias to $\Delta_\alpha^{\mathrm{arith}}$. Archetypes drawing on them therefore carry a narrower band than their construction-choice uncertainty warrants, and the affected cells concentrate in the pre-1948 cohorts.

7. *Slab* pools hold between two and nine constructions at every BAC and are the smallest of any component, so the construction-choice uncertainty of the largest single contributor to the reported GWP is characterized by the fewest observations. The reported Geometric Standard Deviation (GSD) is correspondingly conservative in the downward direction.

8. Component areas are computed once from median archetype geometry, so the TABULA wall ratio $r_{s,b,\ell}$ is evaluated at the single size bin ℓ implied by $\tilde{A}_{l,\alpha}$. The buildings within an archetype span several bins, and the $A_l > 400\,\mathrm{m}^2$ correction is a step, not a gradient (Supplementary Note 2.5), so archetypes whose median living area falls near that threshold do not reproduce the bulk calculation for their own population. This is a property of archetype aggregation and is independent of construction choice.

3.6 Scope of the sensitivity analysis

The procedure above quantifies one specific uncertainty, the construction-choice uncertainty within the construction data pool under a uniform prior, and a related estimator bias computable analytically from the same pool. Three further uncertainty sources are not captured here.

1. Materials that dominate the German stock need not appear in our data pool in proportion to their market share, so the stock-level expectation under actual material prevalence could sit anywhere within the *min*/*max* bounds. No procedure internal to the data pipeline can test this.

2. Inter-state differences in $\widehat{\mathrm{GWP}}_\alpha^{(d,r)}$ reflect geometry only and regional material prevalence is invisible.

3. Uncertainty in the ETHOS.BUILDA geometric attributes (Dabrock et al., 2025) is not propagated. Construction-choice uncertainty and geometric uncertainty are quantified separately and do not compound in the reported bands. Uncertainty in component area estimation (TABULA wall ratios, square-perimeter Wall2, 35° roof pitch, 2.5 m storey height) and in the 50-year reference study period convention is out of scope of the MC procedure.

The geometric mean remains the preferred point estimate because it requires no distributional assumption about the pool, down-weights outlier constructions relative to the arithmetic mean, and produces a conservative estimate relative to the uniform-prior expectation. The systematic gap $\Delta_\alpha^{\mathrm{arith}}$ is reported alongside the point estimate as a quantified uncertainty margin.

3.7 Monte Carlo Sensitivity

Supplementary Table 11 disaggregates the archetype-level MC construction-choice uncertainty by the eleven BAC cohorts and four size classes. Each row reports the geometric-mean point estimate $\overline{\mathrm{GWP}}$ (Supplementary Equation (29)), the deterministic *Min* and *Max* bounds, the uniform-mode bootstrap percentiles P05, P50, and P95, and the coefficient of variation. The *Min* and *Max* columns are the direct analogue of the sub-scenarios presented in Meier-Dotzler (2023), which apply the minimum and maximum eligible construction intensity across the same modules the status quo scenario.

Supplementary Table 11: MC-derived assembly-choice uncertainty of embodied GWP by BAC and size class. Values are unweighted medians across federal states contributing to each cell.

BAC	Size	$\overline{\text{GWP}}$[a]	Min	Max	P05	P50	P95	CV
BAC1	SFH	4.3	2.0	8.9	3.7	5.3	7.0	0.18
	TH	4.4	2.1	9.1	3.8	5.4	7.0	0.18
	MFH	4.1	1.9	8.6	3.2	5.0	7.0	0.23
	AB	3.1	1.5	6.2	2.5	3.7	5.1	0.22
BAC2	SFH	5.6	3.2	9.2	4.7	6.2	7.5	0.13
	TH	5.4	3.2	8.7	4.6	5.9	7.2	0.13
	MFH	5.3	3.0	8.8	4.3	6.1	7.6	0.20
	AB	4.0	2.6	6.4	3.3	4.5	5.7	0.17
BAC3	SFH	7.7	4.0	14.5	6.8	8.5	10.2	0.12
	TH	7.2	3.9	13.7	6.4	7.9	9.6	0.12
	MFH	5.9	3.0	12.0	5.0	6.5	8.7	0.15
	AB	4.6	2.8	8.3	4.0	5.0	6.3	0.14
BAC4	SFH	8.1	4.2	15.2	7.2	8.8	10.5	0.12
	TH	7.6	4.0	14.4	6.8	8.2	9.8	0.11
	MFH	6.4	3.4	12.8	5.6	6.8	8.6	0.13
	AB	4.9	2.8	8.8	4.2	5.2	6.3	0.13
BAC5	SFH	8.3	4.6	15.1	7.5	8.9	10.6	0.11
	TH	7.8	4.3	14.3	7.0	8.4	9.9	0.11
	MFH	6.6	3.6	12.8	5.7	7.0	8.7	0.13
	AB	5.0	3.0	8.7	4.2	5.3	6.4	0.13
BAC6	SFH	8.8	4.9	19.1	7.2	9.8	14.6	0.25
	TH	8.1	4.3	17.7	6.5	9.2	13.7	0.23
	MFH	5.8	3.4	12.3	4.9	6.4	8.9	0.20
	AB	5.0	3.0	9.8	4.3	5.5	7.2	0.17
BAC7	SFH	8.6	4.8	19.2	7.3	9.3	14.4	0.23
	TH	8.3	4.7	17.9	7.1	8.9	13.3	0.20
	MFH	6.5	3.7	13.7	5.6	7.0	10.1	0.18
	AB	5.0	3.0	9.7	4.3	5.4	7.1	0.15
BAC8	SFH	9.4	7.3	14.4	8.3	10.1	12.4	0.14
	TH	9.5	7.4	14.3	8.5	10.0	12.1	0.11
	MFH	6.9	5.2	11.0	6.1	7.5	9.1	0.12
	AB	5.3	4.2	8.4	4.8	5.6	6.9	0.10
BAC9	SFH	9.6	3.8	20.1	7.7	11.1	14.7	0.18
	TH	8.9	3.6	18.8	7.2	10.5	14.1	0.19
	MFH	7.1	2.6	15.6	5.6	8.4	11.3	0.20
	AB	5.3	1.9	11.9	4.0	6.4	9.0	0.23
BAC10	SFH	9.6	3.9	19.6	7.8	11.0	14.3	0.17
	TH	8.8	3.6	18.3	7.2	10.3	13.3	0.18
	MFH	7.5	2.9	15.7	6.0	8.6	11.4	0.19
	AB	4.8	1.6	10.8	3.6	5.8	8.1	0.26
BAC11	SFH	9.7	4.0	20.1	7.9	11.1	14.6	0.17
	TH	8.6	3.5	17.9	7.1	10.0	13.0	0.18
	MFH	7.0	2.6	15.0	5.6	8.2	10.9	0.19
	AB	5.2	1.7	11.7	3.7	6.2	8.6	0.22

[a] $\overline{\text{GWP}}$ is the geometric-mean point estimate (Supplementary Equation (29)).
All values are in kg CO_2e/(m^2·a), except CV.

Supplementary Note 4 Prospective retrofit scenario

The estimation above describes the standing stock as it was built. This note sets out a prospective extension of it, which asks what it would cost in embodied carbon to bring that stock to a current energy-efficiency standard. The extension reuses the geometry, the component areas and the age classification already established, and changes only the construction intensities applied to the components that a retrofit touches.

4.1 Notation

All notation follows Supplementary Note 2 unless stated otherwise. Two symbols are introduced here.

- Retrofitted component set: $\mathcal{E} \subset \mathcal{C}$, the components a retrofit touches, referred to below as the shell configuration (Supplementary Equation (36)). Two configurations are evaluated.
- Family-shifted class keys: $k_i^{\mathrm{ren}} = (b_i, \text{RefurbishedBuilding})$ and $k_i^{\mathrm{nb}} = (b_i, \text{NewConstruction})$. A retrofit changes only the construction family σ of the class key, leaving the age class and every geometric input untouched. A key written k_i without a superscript carries $\sigma = \text{OldBuilding}$, as throughout the baseline.

4.2 The retrofit construction family and its module boundary

We organize structural constructions into three families. The *OldBuilding* family used throughout the baseline describes age-typical construction as built. The *RefurbishedBuilding* family describes the same constructions after an energetic renovation to the KfW-55 standard, and the *NewConstruction* family describes replacement construction and is used here only for windows, for the reason given below.

The *RefurbishedBuilding* family carries a different module boundary from the *OldBuilding* family, and the difference is central to how the scenario must be computed. For a retrofitted component, we account for the disposal (C3–C4) of the layers removed to carry out the work, the production (A1–A3) of the layers newly installed *and of those alone*, the replacement (B4) of the whole post-retrofit construction over the following 50 years, and the disposal (C3–C4) of that construction at the end of them. The production of layers that remain in place is deliberately not counted. Those emissions were released when the building was built and are not incurred again by the decision to retrofit.

A worked example makes the boundary concrete. Insulating a masonry exterior wall from outside adds an insulation layer and a new render or cladding. The scenario counts the production of the insulation and the cladding, the disposal of any surface layer stripped to fit them, the replacement of both over the next 50 years, and the disposal of the whole wall at the end of that period. It does not count the production of the masonry, which was emitted decades earlier. In consequence, a retrofitted component is represented by the *RefurbishedBuilding* intensity *instead of* the *OldBuilding* intensity and not in addition to it, since the retrofit intensity already carries the forward-looking modules of the entire component.

4.3 Which components are retrofitted

We develop retrofit constructions only for components of the heat-transferring envelope, on the grounds that renovating interior walls or intermediate floors does not reduce heat demand. Whether a given envelope component lies on that boundary depends on which parts of the building are heated. We assume an unheated attic and an unheated cellar, which places the boundary at the top-floor ceiling rather than the pitched roof, and at the cellar ceiling rather than the baseplate. The retrofitted set is therefore

$$\mathcal{E} = \{\text{Wall1},\ \text{Window},\ \text{Roof2},\ \text{Floor1}\} \subset \mathcal{C}, \tag{36}$$

that is the exterior wall above ground, the windows, the top-floor ceiling and the cellar ceiling. This matches the definition of a full renovation in the German federal buildings strategy, which comprises the exterior envelope, the roof, the floor and the windows (Thamling et al., 2022). Choosing the top-floor ceiling rather than the pitched roof also keeps the scenario on the same components as the baseline, so that the difference between them is attributable to the retrofit and not to a change of system boundary. The alternative assumption of a heated attic, which moves the boundary to the pitched roof, is reported in Supplementary Note 5.7.

Windows are a special case. Our database provides no retrofit construction for them, because a renovation to this standard replaces windows outright rather than upgrading them. A retrofitted window is therefore represented by the disposal of the existing window at its age-class intensity, followed by the full life cycle of a new-build window:

$$\mathrm{gwp}^{\mathrm{Window}}_{\mathrm{retrofit}} = \mathrm{gwp}^{\text{C3-C4}}_{\mathrm{Window},k_i} + \mathrm{gwp}^{\text{A1-A3}}_{\mathrm{Window},k_i^{\mathrm{nb}}} + \mathrm{gwp}^{\mathrm{B4}}_{\mathrm{Window},k_i^{\mathrm{nb}}} + \mathrm{gwp}^{\text{C3-C4}}_{\mathrm{Window},k_i^{\mathrm{nb}}}. \tag{37}$$

Both the old and the new window carry a frame material. We pair them by frame type and by reported bound, so that an aluminium-framed old window is replaced by an aluminium-framed new one and a minimum-impact old window by a minimum-impact new one. This keeps one representative construction per frame type and bound, exactly as the baseline selection does. Pairing every old frame with every new frame instead would widen the window range from 145.1 to 249.9 kg CO_2e per square meter at the oldest age class, and by about 2% from the third age class upward.

4.4 Building-level accounting

For a retrofitted building i, components inside $\mathcal{E}$ take their retrofit intensity and components outside it keep the forward-looking modules of their as-built intensity:

$$\begin{aligned}\mathrm{GWP}_i^{\mathrm{retrofit}} = &\sum_{c\in\mathcal{E}} A_{c,i}\left(\mathrm{gwp}^{\text{A1-A3}}_{c,k_i^{\mathrm{ren}}} + \mathrm{gwp}^{\mathrm{B4}}_{c,k_i^{\mathrm{ren}}} + \mathrm{gwp}^{\text{C3-C4}}_{c,k_i^{\mathrm{ren}}}\right)\\ &+\sum_{c\notin\mathcal{E}} A_{c,i}\left(\mathrm{gwp}^{\mathrm{B4}}_{c,k_i} + \mathrm{gwp}^{\text{C3-C4}}_{c,k_i}\right)\end{aligned} \tag{38}$$

The first sum runs over the retrofitted components and the second over those retained. The product stage of the as-built construction, $\mathrm{gwp}^{\text{A1-A3}}_{c,k_i}$, appears nowhere in Supplementary Equation (38). It is the *sunk* slice of Supplementary Equation (20), already released, and it is neither re-incurred by a retrofit nor avoided by one. It is reported separately and is never added to the scenario total.

We refer to $\mathrm{GWP}_i^{\mathrm{retrofit}}$ as the *scenario embodied emissions* of building i. The wording is deliberate, and it is not a commitment to any one scenario. The retrofit decision is taken at one moment, but the emissions it entails accrue over the following 50 years: the production of the new layers and the disposal of what is stripped out arise at once, replacement arises across the service life, and the disposal of the whole construction arises at the end of it. The quantity is therefore not what is emitted within any particular window, but what the decision sets in train.

4.5 Selection and pooling of retrofit intensities

Retrofit intensities are selected exactly as the baseline module range is (Supplementary Equation (3)): for each component and age class, the candidate pool comprises the minimum- and maximum-impact construction of every retrofit construction type serving that component, and the pool is ranked once on the A1–C4 total. One selection is used for all reported quantities.

We deliberately do not select on the product stage alone, although that quantity is of obvious interest for a scenario compared against a budget with a fixed end year. Of the 220 component-and-age combinations in the retrofit database, 109 carry a negative product stage, because the retrofit constructions make heavy use of wood-fibre insulation boards and wood-based cladding, which store biogenic carbon at production and release it again at end of life under the rules of DIN Deutsches

Institut für Normung e. V. (2022). Selecting or reporting on the product stage in isolation would therefore book the storage while omitting the release, and would show the retrofit of several component and age combinations as carbon-negative. Every one of the 220 A1–C4 totals is positive, ranging from 8.8 to 273.5 kg CO_2e per square meter of component, so the full total is well behaved where its product-stage part is not.

Where several construction types serve one component, all are pooled, as in the baseline. ETHOS carries no attribute for the load-bearing material of a building, so a timber and a masonry variant of the same component cannot be distinguished and both remain in the pool. The one exception is the roof, which is conditioned on the roof-shape attribute in the same way as the baseline. Our construction pools are in any case already differentiated by age class in a way that follows construction history, so a variant is offered only for age classes in which that construction was actually built.

4.6 Which buildings are retrofitted, and in what order

The scenario applies an annual retrofit rate to the national net floor area, expressed as full-renovation equivalents, and accumulates it from 2025 to 2045 inclusive, a window of 21 years. The window is matched to that of Woytowicz et al. (2025), whose budget covers interventions occurring between those years, so that the two sides of the later comparison describe the same set of events. It carries no temporal meaning of its own: it enters the calculation only through the product rate × years, which fixes the share of the stock treated, and not through any dating of individual retrofits. This is why a wave spanning 21 years can be priced with constructions whose reference service period is 50 years, since the 50-year clock starts at the moment each building is retrofitted rather than at the start of the window. Five rates are evaluated, 0.5 to 2.5% per year in steps of 0.5, spanning the range between rates observed in Germany over the past two decades and those prescribed by federal strategy. No rate is privileged: the grid is a sensitivity across a plausible interval and not a forecast.

Eligibility follows the ETHOS.BUILDA refurbishment attribute, which uses the TABULA schema and labels every building *existing*, *usual* or *advanced* (Dabrock et al., 2025). These correspond to the categories *not refurbished*, *partially refurbished* and *fully refurbished* that Metzger et al. (2019) report at federal-state level. Buildings in the *existing* state are treated first, those in the *usual* state once the first group is exhausted, and those in the *advanced* state never. A second rule applies to every scenario: buildings completed after the 2002 energy-saving ordinance (BAC9 to BAC11) were built to that standard and are placed last in priority, behind the whole pre-2002 stock in either state. At the rates tested they are never reached. Because that attribute is assigned probabilistically and identifies no individual building (Dabrock et al., 2025; Metzger et al., 2019), the rate is applied to a share of floor area and the results are stock-level quantities throughout.

Within the eligible pool, four scenarios are evaluated, which differ only in the order buildings are treated: by construction age from oldest to newest (Scenario 1), by size group taking multi-family houses and apartment buildings before single-family and terraced houses (Scenario 2), at random with a fixed seed (Scenario 3), and a combination of the first two that treats the oldest cohort first and, within each cohort, the larger size group first (Scenario 4). The four are bounding cases chosen to span the range of outcomes a sequencing rule can produce, and are not policy recommendations. Since the retrofitted floor area depends only on the rate, the four scenarios treat identical quantities of floor area at a given rate and differ only in which buildings that area belongs to.

4.7 Comparison with a sector carbon budget

The scenario total is compared against the embodied-carbon budget that Woytowicz et al. (2025) allocate to the German building sector for 2025 to 2045. Their budget downscales the remaining global budget for a 1.7 °C target to Germany on an equal-per-capita basis, then to the building sector on its share of national emissions, then to the embodied share of sector emissions. Executing their published code with their own parameters gives 489.94 Mt CO_2e, which we quote as 490 Mt. Two alternative

global-to-national allocations in the same source, based on current emissions and on gross domestic product, give 827.3 and 1,881.2 Mt CO_2e respectively.

The two sides of this comparison are commensurable, which is what makes it admissible. The budget covers the same life-cycle modules that we compute, namely A1–A3, B4 and C3–C4. It applies to interventions occurring within the same window. And it treats each intervention over its whole life cycle rather than counting only the part falling before the end year, so that a comparison against a total accruing over 50 years is like for like. Their scope is broader than ours in one respect that works against our own conclusion: their budget must cover new construction as well as renovation, and non-residential as well as residential buildings, so residential retrofit alone is a strict subset of what the budget has to accommodate and any share we report is conservative.

Supplementary Note 5 Extended results

This note reports results that extend those in the corresponding article without being essential to its central argument. It is organized in three parts. The first extends the baseline account of the standing stock: embodied carbon across the sixteen federal states (Supplementary Note 5.1), the component composition of per-area intensity by building size (Supplementary Note 5.2), embodied carbon and stock composition aggregated by settlement type (Supplementary Note 5.3) and the life-cycle module range resolved by construction age (Supplementary Note 5.4). The second documents the retrofit scenario in full: the composition of the stock it draws on together with the complete scenario analysis (Supplementary Note 5.5), and the same analysis under an alternative thermal envelope configuration (Supplementary Note 5.7). The third validates the approach against an independent case study (Supplementary Note 5.8) and against prior life-cycle studies (Supplementary Note 5.9).

5.1 Embodied carbon by federal state

Supplementary Table 12 reports the embodied-GWP distribution for each federal state, ordered by ascending mean, alongside the size-class and age-cohort composition of each state's stock. State means span 5.65 in Saxony to 8.37 in Schleswig-Holstein, a 1.5-fold spread around the national mean of 7.16 (median 7.19). The ordering is not neutral with respect to data provenance: the six states whose building heights are modeled from OpenStreetMap instead of three-dimensional city models, namely Schleswig-Holstein, Baden-Württemberg, Rhineland-Palatinate, Bremen, Saarland and Mecklenburg-Western Pomerania, occupy the six highest means (8.37, 8.29, 8.29, 8.28, 8.26 and 7.51), while the highest three-dimensional-model state, Lower Saxony, sits at 7.43. Because the same construction families and area model apply everywhere, this clustering points to the OpenStreetMap-based height model of those six states and not to genuine regional differences in construction. As detailed in Supplementary Note 2.2, this source-level heterogeneity is not something the present workflow can correct, and the appropriate remedy is a future ETHOS.BUILDA release on a uniform, sixteen-state LoD2 basis. At the other end, the three lowest-mean states, Saxony (5.65), Thuringia (5.67) and Saxony-Anhalt (5.82), each carry roughly 64% of their stock in the pre-war (BAC 1–2) cohort, against a national 18%, and it is the weight of that early construction, of which the pre-1919 lime-mortar *Gründerzeit* stock is the lightest in the country, that pulls their means down.

5.2 Component composition of per-area intensity by size class

Resolving each size class's stock-mean intensity into its structural components confirms that the size ordering reported in the corresponding article is a property of building geometry, not of the constructions used (Supplementary Fig. 3). The enclosing shell of roof, external walls and windows is amortized over less floor area in a small building, so its share of per-area intensity falls from about 48% in a single-family or terraced house to 37% in a multi-family house and 30% in an apartment building. The ground-contact substructure of cellar floor, base plate and foundation falls in step over the same sequence, from about 28% to 15%. The internal structure moves the opposite way. The stacked intermediate floor slabs and interior walls, which recur with every storey, rise from about 24% of a single-family house's intensity to 55% of an apartment building's, where the floor slab alone is the single largest component, at 37% against 18% in a single-family house. A single-family house therefore concentrates its embodied carbon in an enclosing shell spread over little floor area, whereas an apartment building concentrates it in repeated horizontal structure, and the higher per-area intensity of the small building follows from that geometry and not from any difference in the constructions used.

5.3 Embodied carbon and stock composition across settlement types

A building-resolved account can be aggregated to any spatial unit, including units that no coarser dataset can address. The federal-state and district aggregations reported elsewhere in this note follow administrative boundaries. Here we aggregate the same buildings by *settlement type* instead, which

Supplementary Table 12: Descriptive statistics for the analytical sample, by federal state. Size-class and age-cohort columns are percentage shares of the state's building count. The per-m^2·a statistics are stock-level values for floor-area-normalized embodied GWP. States are ordered by ascending mean GWP. All buildings use the *OldBuilding* assembly family.

		Size class	Age cohort	GWP [kg CO_2e/(m^2·a)]			
State	n [Mio.]	SFH/TH/MFH/AB	≤ 48/49–78/79–01/≥ 02[a]	mean	median	P10–P90[b]	min–max
Saxony	0.83m	75.89/3.19/20.47/0.45	63.63/27.10/8.04/1.23	5.65	5.07	3.53–8.54	2.11–23.47
Thuringia	0.70m	84.49/4.04/11.37/0.09	64.97/27.88/6.18/0.97	5.67	5.10	3.75–8.38	2.22–23.12
Saxony-Anhalt	0.81m	81.50/5.15/13.12/0.23	63.70/28.67/6.57/1.06	5.82	5.19	3.80–8.75	2.15–21.69
Berlin	0.26m	55.14/8.29/26.01/10.56	61.79/28.26/6.20/3.75	6.03	5.75	3.06–9.15	1.69–23.20
Bavaria	3.28m	82.09/7.28/9.96/0.67	7.76/81.80/7.92/2.52	6.72	6.65	5.09–8.44	2.09–17.49
Brandenburg	0.74m	88.76/3.50/7.61/0.12	42.18/44.53/10.39/2.90	6.83	6.68	4.34–9.52	2.18–23.39
Hesse	1.85m	78.63/8.55/12.64/0.17	11.04/83.45/3.96/1.55	6.86	6.82	4.96–8.81	2.18–31.36
Hamburg	0.21m	55.54/17.46/26.20/0.81	14.14/79.18/4.34/2.33	7.21	7.13	4.61–9.78	2.21–23.29
N. Rh.-Westph.	4.14m	65.84/12.28/21.75/0.13	7.67/83.78/5.51/3.05	7.27	7.07	5.36–9.33	2.05–48.73
Lower Saxony	2.21m	85.76/5.82/8.36/0.06	12.57/75.62/9.01/2.81	7.43	7.50	4.97–9.62	2.14–24.38
Meckl.-Vorp.	0.25m	78.86/5.31/15.36/0.47	29.28/55.47/11.90/3.35	7.51	8.09	4.55–9.63	2.37–24.40
Saarland	0.27m	82.30/7.34/10.30/0.06	3.55/92.70/2.79/0.95	8.26	8.32	7.08–9.28	3.05–19.95
Bremen	0.12m	31.65/37.08/30.88/0.39	5.99/88.42/3.03/2.56	8.28	8.30	6.14–10.34	2.62–21.66
Rhineland-Pal.	0.95m	83.50/5.62/10.80/0.08	7.29/86.25/4.45/2.01	8.29	8.42	6.65–9.72	2.24–22.83
Baden-Württ.	2.21m	74.77/7.83/17.26/0.14	5.83/86.55/5.01/2.61	8.29	8.40	6.69–9.70	2.44–26.08
Schleswig-H.	0.58m	77.88/9.38/12.64/0.10	8.37/81.68/6.97/2.98	8.37	8.52	6.23–10.13	2.38–22.20
Germany	19.42m	76.87/8.10/14.64/0.39	17.51/73.59/6.49/2.42	7.16	7.19	4.67–9.30	1.69–48.73

[a] Age cohort shares collapse BACs into four eras (BAC1–2, BAC3–5, BAC6–8, BAC9–11).
[b] 10th to 90th percentile of the distribution.

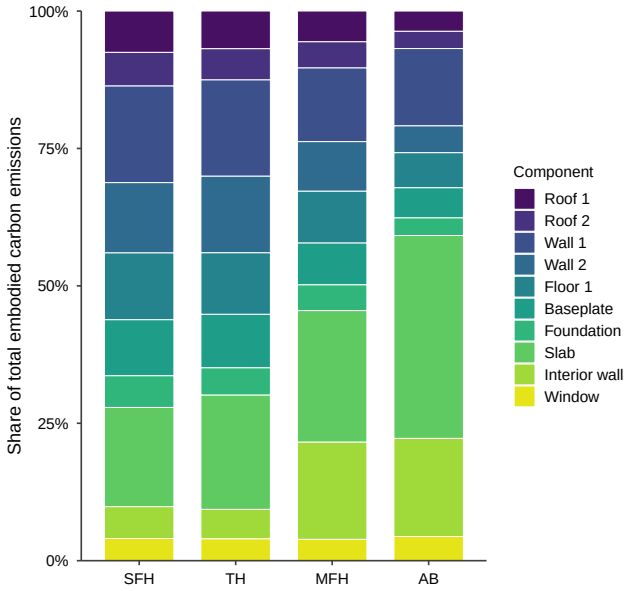
cuts across those boundaries and separates metropolitan cores from rural villages irrespective of which state they lie in. The purpose is to show what the additional spatial resolution reveals, and what it does not.

Supplementary Fig. 4 places every building in one of the seven Regional Statistical Spatial Typology for Mobility and Transport Research (RegioStaR) settlement classes and shows the per-area embodied-carbon distribution (panel c) alongside the size-class (panel a) and age-class (panel b) composition of each class. Two readings follow.

First, the per-area distribution is nearly invariant across the gradient. Class medians span only 6.56 kg CO_2e/(m^2·a) in the metropolitan class to 7.54 in medium-sized cities, about 1 kg CO_2e/(m^2·a) around the national median of 7.19, and there is no monotonic urban-to-rural trend. The metropolitan class carries the lowest median because it holds the largest multi-family and apartment share, whereas the rural classes are almost entirely single-family and sit between 7.02 and 7.18.

Second, the composition panels show why. Within every settlement class the ordering by building size is reproduced, with multi-family houses near 5.7 to 6.8 and single-family houses near 7.0 to 7.6 kg CO_2e/(m^2·a). What differs between classes is the mix of building sizes and ages, not the per-area intensity of any given type. The near-invariance of the class medians is therefore a composition effect, and the same effect is visible at coarser resolution in the state-level values of Supplementary Table 12.

Taken together, these two readings illustrate what a building-resolved account adds. Aggregate statistics at any single spatial level, whether state, district or settlement class, compress two distinct quantities into one number: the intensity of each building type, and the local mix of types. Only an



Supplementary Figure 3: **Component composition of embodied carbon by size class.** Share of the stock-mean per-area intensity attributable to each structural component, for single-family (SFH), terraced (TH) and multi-family (MFH) houses and apartment buildings (AB). Bars sum to 100% within each size class.

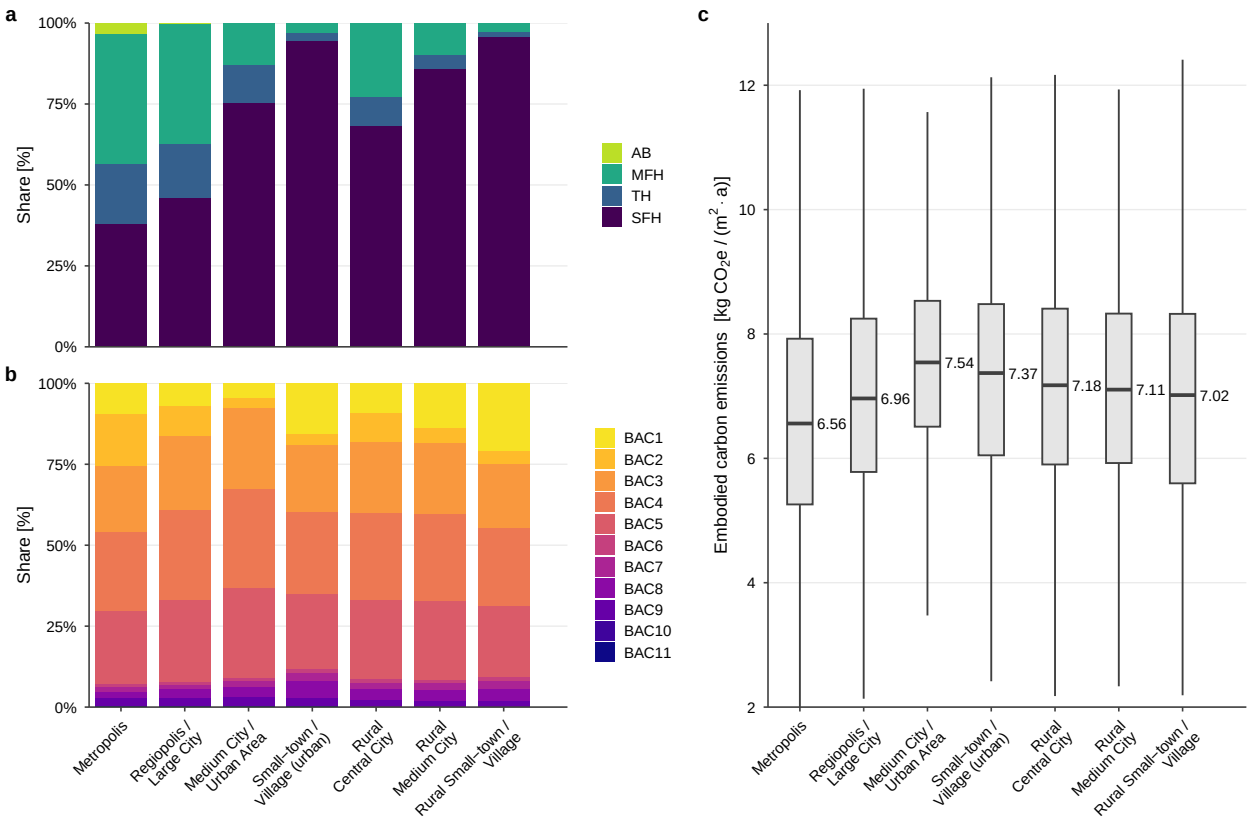
account resolved to individual buildings can separate them, and the separation matters for targeting, because a policy addressed to a settlement class implicitly addresses whichever building types happen to be common there.

5.4 Life-cycle module range by construction age

The module range introduced in the corresponding article is the additive minimum–maximum range obtained by assigning every component the minimum- and maximum-impact representative construction of its age class. It is reported by building size in the corresponding article and resolved here by construction age (Supplementary Table 13). The national range is 3.19–11.55 kg CO_2e/(m^2·a), of which the product stage (A1–A3) contributes 1.17–8.59, the recurring replacement flow (B4) 0.08–0.72, and the end-of-life flow (C3–C4) 1.94–2.24. Because each column is read from a single construction, the three module groups sum to the total within a column, and almost all of the spread is carried by the product stage. Across age classes, the product-stage minimum turns negative for the oldest cohort (BAC 1) and the three most recent (BAC 9–11). There the minimum-impact construction of several components is timber-based and books biogenic carbon as stored at the product stage and released at end of life, so the forward flow (B4 + C3–C4) exceeds the total and an individual module group runs opposite to the A–C total on which the two representative constructions are selected. The width of the range itself varies with construction age. The mid-century cohorts that dominate the stock carry ranges of roughly 3 to 12 kg CO_2e/(m^2·a), whereas the most recent cohorts (BAC 9–11) span 2.2 to about 19.0, because their minimum-impact construction is timber-based and their maximum-impact construction is mineral. In these recent cohorts the end-of-life flow (C3–C4) runs from about 4.4 to 11.6, far above the 1.9 to 2.2 of the stock as a whole.

5.5 Retrofit scenario: stock composition and the complete scenario analysis

The retrofit scenario applies EH-55 constructions to the exterior walls, windows, roof and floor of the standing stock at five annual rates and under four scenarios, which differ only in the order buildings are treated. Supplementary Table 14 reports the composition of the stock those scenarios



Supplementary Figure 4: **Embodied carbon across the RegioStaR settlement-type gradient.** The seven RegioStaR classes comprise four urban levels (Metropolis, Regiopolis/Large City, Medium City/Urban Area, Small-town/Village urban) and three rural levels (Rural Central City, Rural Medium City, Rural Small-town/Village). Panels (a) and (b) share the class axis and show stock composition by size class and by age class, respectively, as percentage shares of each class's stock. Panel (c) shows the embodied-GWP distribution in kg CO_2e/(m^2·a). Whiskers extend to 1.5× the interquartile range, and outliers are suppressed for legibility.

draw on. Eligibility for retrofitting follows the ETHOS.BUILDA refurbishment attribute, which labels each building into refurbishment states *existing*, *usual* or *advanced*. *Existing* indicates unrefurbished. Buildings in the *existing* state (38.4% of total national NFA) are treated first and those in the *usual* state (56.5%) once the first group is exhausted, while the *advanced* state (5.1%) is never retrofitted. Also, buildings completed after the 2002 energy-saving ordinance in Germany are placed last in priority, as they represent buildings with better energy performance. The two conditions combine into the eligibility ladder shown in Supplementary Table 14, which leaves a reachable pool of 4,352.0 Mm^2 across 18,171,268 buildings, 94.0% of the national total. The same ladder applies to all four scenarios, so they draw on one pool and differ in the order they work through it. The size ordering groups multi-family houses and apartment buildings together, which is 34.1% of national NFA, ahead of single-family and terraced houses at 65.9% (Supplementary Table 6).

Supplementary Table 15 reports every one of the 20 scenario combinations behind Fig. 4 of the corresponding article. We highlight two things here. First, the retrofitted floor area depends only on the rate, so the four scenarios in a given row of the rate column treat exactly the same quantity of floor area and differ only in which buildings that area belongs to. Second, the spread between the four scenarios is not uniform across rates, and it is smallest in the middle of the interval. Measured at the minimum-impact construction, the four scenarios differ by 51% at 0.5%/a, 16% at 1.0%/a, 5% at 1.5%/a, 8% at 2.0%/a and 15% at 2.5%/a. At the low end they disagree over which small part of

Supplementary Table 13: Life cycle modules of the German residential building stock, by building age class. All quantities are in kg CO_2e/(m^2·a), weighted by NFA and annualized over the reference service life. Columns headed *min.* and *max.* give the values obtained when every component is assigned the minimum- and the maximum-impact construction of its age class, following Supplementary Equations (3), (4) and (21).

		Total		A1–A3		B4		C3–C4	
BAC[a]	n [Mio.]	min.	max.	min.	max.	min.	max.	min.	max.
1	2.27	1.44	7.80	−2.61	4.01	0.04	0.40	4.00	3.39
2	1.13	2.90	9.52	0.87	7.12	0.06	0.23	1.97	2.17
3	4.29	3.07	12.52	1.48	9.86	0.07	0.81	1.52	1.85
4	5.24	3.39	12.04	1.60	9.54	0.07	0.81	1.72	1.69
5	4.76	3.88	11.97	2.50	9.22	0.07	0.72	1.32	2.03
6	0.23	3.79	13.61	2.79	12.08	0.12	0.71	0.88	0.83
7	0.37	3.83	14.30	2.79	11.94	0.12	1.00	0.92	1.36
8	0.66	6.50	11.89	4.89	8.85	0.35	1.37	1.26	1.67
9	0.41	2.22	18.97	−2.62	6.48	0.47	0.88	4.37	11.61
10	0.03	2.34	18.38	−2.83	6.15	0.48	0.90	4.68	11.34
11	0.03	2.36	18.35	−2.82	6.02	0.48	0.92	4.71	11.42
All	19.42	3.19	11.55	1.17	8.59	0.08	0.72	1.94	2.24

[a] BAC definitions follow Supplementary Table 2.
Because each column is read from a single construction, A1-A3, B4 and C3-C4 sum to the total in the same column, and the age class rows aggregate by NFA to the national row. The two constructions are selected on the A-C total, so an individual module group may run opposite to it. This occurs at BAC1, where the minimum-impact constructions are timber-based and carry a higher end-of-life release than the mineral constructions that set the maximum. Negative A1-A3 values arise where the minimum-impact constructions of several components store biogenic carbon at the product stage, which is released in C3-C4.

the stock is treated at all, so the choice of sequence makes most of the difference. As the treated share grows the mix of buildings converges and the scenarios more and more agree. At the maximum-impact construction end they diverge again, because they exhaust the *existing* state at different rates and begin drawing on the *usual* state at different points.

Retrofit constructions are derived from as-built constructions, so applying them to buildings already in the *usual* state counts insulation that may already be present. The first tier of the ladder (Supplementary Table 14) is exhausted only above 1.80%/a, so no run at or below 1.5%/a reaches the *usual* state and those runs are free of this caveat. Where it is reached, however, it accounts for 7.8 to 12.1% of the scenario total at 2%/a and 22.9 to 30.6% at 2.5%/a, depending on the scenario. However, as this group of buildings was built before 2002 and most of the stock in all size classes sits in BAC 4 and older (see Supplementary Table 2), any one of these buildings will likely be retrofitted again in the future, so we assume these buildings will be retrofitted to the EH 55 standard in the future as well.

5.6 Where the scenario's embodied carbon sits across the life cycle

Supplementary Fig. 5 resolves the scenario total into its three module groups. Most of the embodied carbon a retrofit produces is not released when the actual retrofit work is carried out. Taking Scenario 4 at 2%/a, which produces 305 to 549 Mt CO_2e in total, producing and installing the new layers accounts for 52 to −141 Mt, replacing them over the following 50 years for 45 to 46 Mt, and disposing of them

Supplementary Table 14: **Composition of the German residential building stock, as used by the retrofit scenario.** Net floor area by construction-age class, size class and refurbishment state. These shares determine which buildings are eligible for retrofit in each scenario run and the order in which they are treated. The lower block gives the eligibility ladder, which applies identically to all four scenarios.

Group	n[a]	NFA [Mm^2][b]	Share of NFA [%]
By construction-age class [c]			
BAC1	2,266,550	708.5	15.3
BAC2	1,133,140	217.5	4.7
BAC3	4,288,236	1001.9	21.6
BAC4	5,238,524	1223.3	26.4
BAC5	4,764,084	1112.0	24.0
BAC6	228,101	67.9	1.5
BAC7	369,407	103.7	2.2
BAC8	663,170	118.1	2.5
BAC9	414,492	67.5	1.5
BAC10	25,296	4.6	0.1
BAC11	29,623	5.5	0.1
By size class			
SFH	14,928,996	2840.9	61.4
TH	1,573,265	209.5	4.5
MFH	2,843,328	1409.1	30.4
AB	75,034	171.0	3.7
By size group, as used for the size ordering			
MFH+AB	2,918,362	1580.1	34.1
SFH+TH	16,502,261	3050.4	65.9
By refurbishment state [d]			
existing	7,412,410	1780.0	38.4
usual	11,023,316	2615.7	56.5
advanced	984,897	234.9	5.1
By eligibility tier, in the order the scenario treats them			
Tier 1 (BAC1–8, *existing*)	7,230,476	1749.6	37.8
Tier 2 (BAC1–8, *usual*)	10,758,858	2572.1	55.5
Tier 3 (BAC9–11, *existing*)	181,934	30.3	0.7
Not eligible	1,249,355	278.5	6.0

[a] n is the count of individual buildings in the group.
[b] Net floor area in millions of square meters. *Share of NFA* is that area as a percentage of the 4,630.5 Mm^2 national total across all 19,420,623 buildings.
[c] As defined in Supplementary Table 2.
[d] Refurbishment state is an ETHOS.BUILDA attribute and labels each building *existing* (1), *usual* (2) or *advanced* (3) (Dabrock et al., 2025). Every scenario retrofits *existing* first, then *usual*, and never *advanced*.

at the end of that period for 207 to 644 Mt, which is visible in the life-cycle module decomposition in

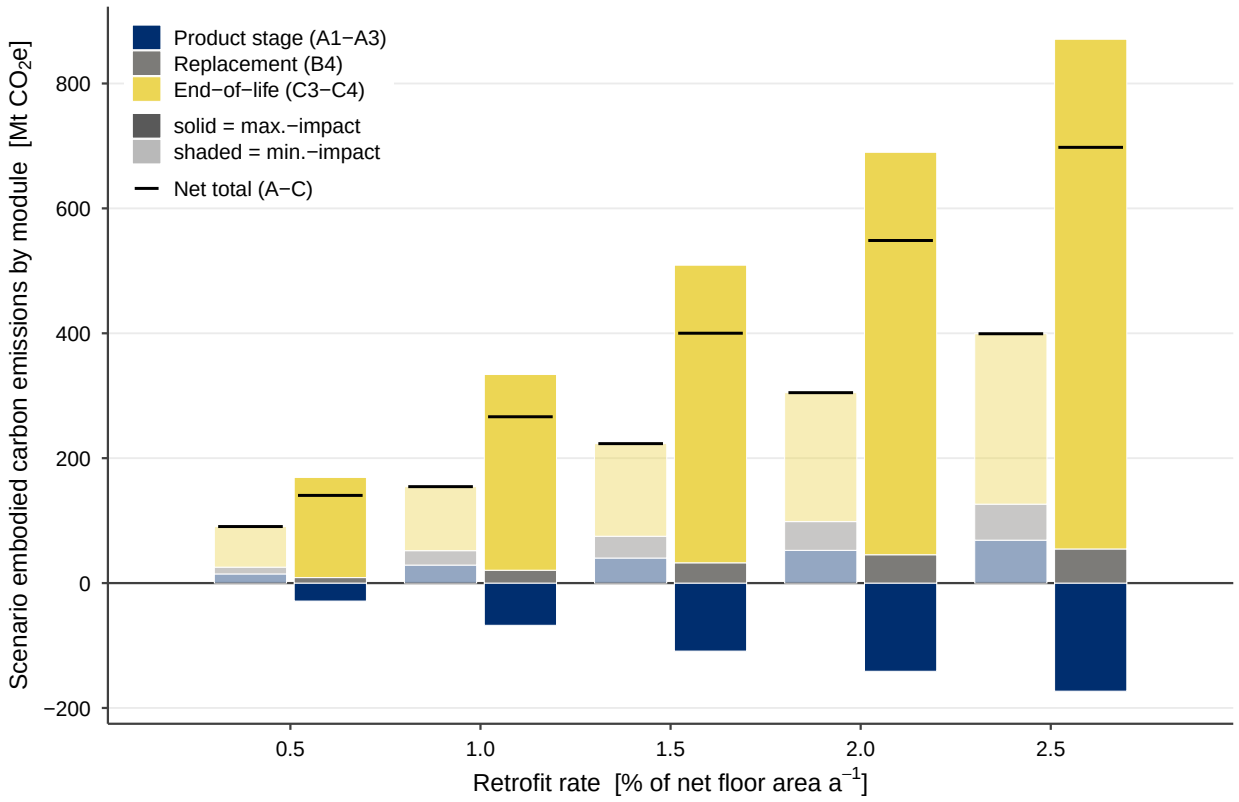
Supplementary Table 15: **Retrofit scenarios: unheated attic and cellar, configuration used in the corresponding article.** Retrofitted components are Wall1, Window, Roof2 and Floor1.

Scenarios[a]	Rate[b]	NFA retrofitted [c]		Scenario total[d]	Share of budget[e]	Increment[f]
	[%/a]	[Mm^2]	[%]	[Mt CO_2e]	[%]	[Mt CO_2e]
Scenario 1	0.5	486	10.5	93.0–148.5	19.0–30.3	22.3–71.3
	1.0	972	21.0	157.6–273.3	32.2–55.8	45.8–133.4
	1.5	1,459	31.5	225.8–407.0	46.1–83.1	75.7–203.0
	2.0	1,945	42.0	309.4–559.4	63.1–114.2	100.3–280.1
	2.5	2,431	52.5	402.4–707.9	82.1–144.5	125.0–353.2
Scenario 2	0.5	486	10.5	61.5–103.7	12.6–21.2	18.8–48.7
	1.0	972	21.0	136.2–245.2	27.8–50.0	45.6–121.1
	1.5	1,459	31.5	215.2–399.3	43.9–81.5	75.2–201.3
	2.0	1,945	42.0	287.4–533.4	58.7–108.9	100.4–269.0
	2.5	2,431	52.5	349.5–637.7	71.3–130.2	119.2–318.0
Scenario 3	0.5	486	10.5	73.0–136.6	14.9–27.9	25.8–69.3
	1.0	972	21.0	145.9–273.3	29.8–55.8	51.6–138.6
	1.5	1,459	31.5	218.8–409.9	44.7–83.7	77.5–207.9
	2.0	1,945	42.0	292.2–546.9	59.6–111.6	103.3–277.4
	2.5	2,431	52.5	366.5–685.0	74.8–139.8	129.1–347.4
Scenario 4	0.5	486	10.5	90.5–140.4	18.5–28.6	21.1–66.7
	1.0	972	21.0	154.4–266.3	31.5–54.4	44.3–129.3
	1.5	1,459	31.5	223.3–400.1	45.6–81.7	74.0–198.7
	2.0	1,945	42.0	304.9–548.6	62.2–112.0	98.5–272.6
	2.5	2,431	52.5	399.2–697.8	81.5–142.4	123.5–347.5

[a] Scenarios: *Scenario 1*, sorted by construction-age class from oldest to newest, *Scenario 2*, multi-family houses and apartment buildings before single-family and terraced houses, *Scenario 3*, drawn irrespective of age or size, and *Scenario 4*, oldest age class first with larger buildings treated first within each class.
[b] *Rate* is the annual retrofit rate as a percentage of national net floor area (NFA), applied from 2025 to 2045 inclusive.
[c] *NFA retrofitted* is the floor area treated over that period, which depends on the rate alone and is therefore identical across the four scenarios at a given rate.
[d] *Scenario total* is the embodied carbon the retrofitted stock produces over the 50 years following each retrofit, covering life-cycle modules A1–A3 (product stage), B4 (replacement) and C3–C4 (end of life).
[e] *Share of budget* expresses it against the 489.94 Mt CO_2e embodied budget allocated to the German building sector for 2025–2045 (Woytowicz et al., 2025).
[f] *Increment* is the part attributable to the retrofit itself. The remainder is carbon the untouched components of the same buildings carry whether or not the retrofit happens.
Ranges written x–y span the minimum- to maximum-impact construction of the relevant component pools.

Supplementary Fig. 5.

Expressed as shares, the result is the opposite of the standing stock's. At the upper bound (maximum-impact construction) the standing stock holds 74% of its embodied carbon in the product stage, 6% in replacement and 19% at end of life (Supplementary Table 13), whereas the retrofit holds −26% in the product stage, 8% in replacement and 118% at end of life (Supplementary Fig. 5). The standing stock's embodied carbon is dominated by production that has already happened. A retrofit's



Supplementary Figure 5: **Life-cycle module decomposition of the embodied carbon of a EH-55 retrofit of the standing stock.** Paired diverging stacked bars give the three module groups at each annual retrofit rate. Shaded bars are the minimum-impact and solid bars the maximum-impact construction of the A1–C4 total, and the black tick marks the net A1–C4 total of each bar. Drawn for Scenario 4, the order that treats the oldest construction cohorts first with larger buildings ahead of smaller ones within each cohort. A1–A3 falls below zero at the upper bound because the retrofit constructions contain wood-fiber insulation, which books biogenic uptake in A1–A3 and the corresponding release in C3 at year 50. This decomposition shows the unheated-attic configuration used in the corresponding article.

is dominated by an end of life that has not yet arrived.

Retrofit constructions make heavy use of wood-fiber insulation. Under the biogenic-carbon rules of DIN EN 15804:2022-03 (DIN Deutsches Institut für Normung e. V., 2022), which govern the environmental product declarations the database is built from, the uptake is booked in A1–A3 and the corresponding release in C3. At the upper bound the uptake exceeds the fossil production emissions of the whole retrofit stack, so A1–A3 falls below zero while the release appears in C3–C4 at year 50.

5.7 Retrofit scenario under the heated-attic configuration

The Results section of the corresponding article assumes an unheated attic and an unheated cellar, so the thermal boundary at the top of the building is the top-floor ceiling (Roof2) and thus the retrofitted component set is Wall1, Window, Roof2 and Floor1. That choice keeps the scenario on the same components as the baseline, so the difference between them is attributable to the retrofit and not to a change of system boundary. Where the attic is heated the boundary moves to the roof itself (Roof1). Supplementary Fig. 6 and Supplementary Table 16 repeat the full scenario analysis under this alternative assumption.

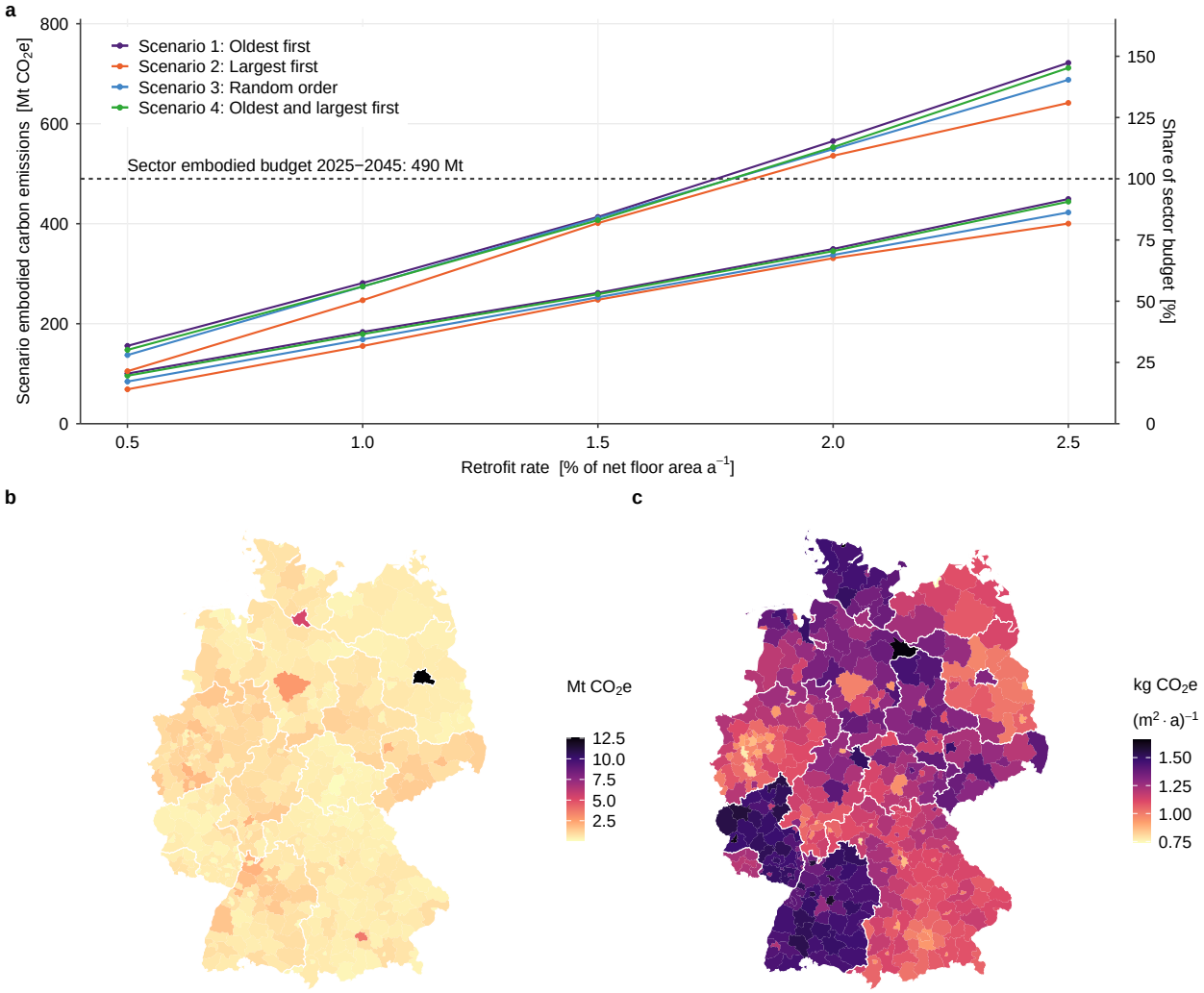
The heated-attic variant is consistently more carbon intensive. Under the oldest-first scenario it

Supplementary Table 16: **Retrofit scenarios: heated attic, supplementary variant.** Retrofitted components are Wall1, Window, Roof1 and Floor1. Roof1 replaces the top-floor ceiling (Roof2) as the thermal boundary.

Scenarios[a]	Rate[b]	NFA retrofitted [c]		Scenario total[d]	Share of budget[e]	Increment[f]
	[%/a]	[Mm^2]	[%]	[Mt CO_2e]	[%]	[Mt CO_2e]
Scenario 1	0.5	486	10.5	100.2–155.7	20.5–31.8	29.5–78.4
	1.0	972	21.0	183.5–281.4	37.5–57.4	71.6–141.5
	1.5	1,459	31.5	261.7–413.6	53.4–84.4	111.6–209.6
	2.0	1,945	42.0	349.4–565.3	71.3–115.4	140.3–286.0
	2.5	2,431	52.5	449.4–721.8	91.7–147.3	172.0–367.1
Scenario 2	0.5	486	10.5	68.8–105.0	14.1–21.4	26.0–50.0
	1.0	972	21.0	155.4–246.9	31.7–50.4	64.8–122.8
	1.5	1,459	31.5	247.9–401.2	50.6–81.9	107.9–203.2
	2.0	1,945	42.0	331.0–535.9	67.6–109.4	144.1–271.5
	2.5	2,431	52.5	400.2–641.6	81.7–131.0	170.0–321.9
Scenario 3	0.5	486	10.5	84.3–137.2	17.2–28.0	37.2–69.9
	1.0	972	21.0	168.6–274.4	34.4–56.0	74.3–139.7
	1.5	1,459	31.5	252.8–411.4	51.6–84.0	111.4–209.4
	2.0	1,945	42.0	337.5–549.2	68.9–112.1	148.5–279.7
	2.5	2,431	52.5	422.6–687.9	86.3–140.4	185.3–350.4
Scenario 4	0.5	486	10.5	96.0–147.6	19.6–30.1	26.6–73.9
	1.0	972	21.0	179.2–274.6	36.6–56.0	69.1–137.5
	1.5	1,459	31.5	258.9–407.1	52.9–83.1	109.7–205.7
	2.0	1,945	42.0	345.2–553.1	70.5–112.9	138.8–277.1
	2.5	2,431	52.5	444.1–711.7	90.7–145.3	168.4–361.4

[a] Scenarios: *Scenario 1*, sorted by construction-age class from oldest to newest, *Scenario 2*, multi-family houses and apartment buildings before single-family and terraced houses, *Scenario 3*, drawn irrespective of age or size, and *Scenario 4*, oldest age class first with larger buildings treated first within each class.
[b] *Rate* is the annual retrofit rate as a percentage of national net floor area (NFA), applied from 2025 to 2045 inclusive.
[c] *NFA retrofitted* is the floor area treated over that period, which depends on the rate alone and is therefore identical across the four scenarios at a given rate.
[d] *Scenario total* is the embodied carbon the retrofitted stock produces over the 50 years following each retrofit, covering life-cycle modules A1–A3 (product stage), B4 (replacement) and C3–C4 (end of life).
[e] *Share of budget* expresses it against the 489.94 Mt CO_2e embodied budget allocated to the German building sector for 2025–2045Woytowicz et al. (2025).
[f] *Increment* is the part attributable to the retrofit itself. The remainder is carbon the untouched components of the same buildings carry whether or not the retrofit happens.
Ranges written *x–y* span the minimum- to maximum-impact construction of the relevant component pools.

produces 100.2 to 155.7 Mt CO_2e at 0.5%/a and 451.7 to 736.1 Mt at 2.5%/a, against 93.0 to 148.5 and 403.9 to 721.2 Mt in the configuration used in the corresponding article, an increase of 2 to 12% depending on rate and bound. Insulating a pitched roof requires stripping and replacing the tiles and battens to reach the rafters, whereas insulating a top-floor ceiling does not, and that additional material is what the difference records.



Supplementary Figure 6: **Embodied carbon of retrofitting the standing stock to the EH-55 efficiency standard, assuming a heated attic.** Retrofitted components are the exterior wall (Wall1), windows, the roof (Roof1) and the cellar ceiling (Floor1). This differs from the configuration used in the corresponding article only in the roof: there the attic is unheated, so the thermal boundary is the top-floor ceiling (Roof2) rather than the roof itself. **(a)** Scenario embodied carbon in Mt CO_2e (life-cycle modules A1–C4, accumulated over the 50 years following each retrofit) against the annual retrofit rate in per cent of net floor area per year. One shaded band per scenario, each spanning the minimum- to maximum-impact construction of the relevant component pools. Scenario 1 treats the oldest construction cohorts first, Scenario 2 retrofits multi-family houses and apartment buildings before single-family and terraced houses, Scenario 3 draws at random, and Scenario 4 combines the first two. All scenarios place buildings completed after the 2002 energy-saving ordinance last in priority. The horizontal line marks the 489.94 Mt CO_2e embodied budget allocated to the German building sector for 2025–2045 (Woytowicz et al., 2025), and the right-hand axis reads the same quantity as a percentage of that budget. Panels **(b)** and **(c)** Embodied emissions attributable to the retrofit itself, by county, for Scenario 4 at 2% per year, assuming the highest-impact construction throughout: (b) in absolute terms, and (c) normalized on the county's whole net floor area over the 50-year reference period. Panel b reads as a map of how much building each county contains, and panel c as the allocation each county would carry per unit of its own floor area. The scenario applies a single national retrofit rate with no spatial targeting, so neither map is a prioritization.

Supplementary Table 17: Comparison of the bottom-up GWP estimation for the Moosach district in Munich against results from Meier-Dotzler (2023).

Source	Statistics	GWP [kg CO_2e/(m^2·a)]
Meier-Dotzler (2023)	Min / Max	2.14 / 8.00
This study	Min / Max	2.72 / 9.28

Sample constructed by intersecting the building stock with the identified Meier-Dotzler (2023) case-study area in Moosach, Munich, containing $n_{\text{buildings}} = 275$, which is comparable in scale to the author's case ($n_{\text{buildings}} = 181$). The area is almost entirely multi-family (92% MFHs, 8% ABs). We restrict the sample to the scope of Meier-Dotzler (2023): MFHs built between 1919 and 1968 (BAC2–BAC4), which leaves $n_{\text{buildings}} = 193$ on which our figures are computed.

5.8 Cross-check against a documented case study

Supplementary Table 17 compares our building-level estimates against a published bottom-up assessment that reports results for an identifiable German neighborhood at a compatible scope. The two assessments draw their construction intensities from the same database, so this comparison tests our building-specific geometry and area model, not the pipeline as a whole. Meier-Dotzler (2023) report a minimum–maximum range of 2.14–8.00 kg CO_2e/(m^2·a) for a multi-family case study. Restricting our stock to the same setting, the multi-family buildings of the Moosach district in Munich built between 1919 and 1968 (BAC 2–4, $n = 193$), yields 2.72–9.28 over the same modules. The district is almost entirely multi-family, at 92% multi-family houses and 8% apartment blocks, and our geometric-mean point estimate over its 193 buildings is 4.91 kg CO_2e/(m^2·a), which sits within both the reference range and our own. Both bounds sit modestly above the reference, by 0.6 and 1.3 kg CO_2e/(m^2·a), and the ranges overlap across most of their span. The offset is consistent with our evaluating each building on its own ETHOS.BUILDA geometry instead of a single representative archetype, and with a marginally different sample ($n = 193$ against 181), and not with a difference in intensities, which are shared. The geometry and area model thus reproduce the documented case-study range with only a small upward offset.

5.9 Comparison with prior residential embodied-carbon studies

Supplementary Table 18 situates this study within the residential life-cycle-assessment literature. Prior building-level assessments rest on samples ranging from a single building to a few hundred and infer geometry from typological archetypes rather than from measured per-building form, whereas we evaluate all 19.4 million buildings on their individual geometry. The few assessments that reach stock scale, both for the United States, likewise substitute archetype look-ups for per-building geometry (Hu, 2023; Ghorbany and Hu, 2024). Numerical comparison across the full table is constrained because the studies differ in system boundary, reference area and reference study period, and the widest reported intensities come from assessments of broader scope, including those that add the operational stage (B6). The German studies from DGNB and BPIE (2025) and Meier-Dotzler (2023) are the most directly comparable, sharing the DIN EN 15978 module scope (A1–A3, B4, C3–C4), a 50-year reference study period and a net-floor-area basis, all of which we adopt. Our median of 7.19 sits in the lower-to-middle of the reported German range, and its 1.7–48.7 spread reflects the heterogeneity of a national stock evaluated building by building in place of a few hundred archetypes.

Supplementary Table 18: Residential LCA Studies and Embodied GWP Benchmarks.

Authors	Region	Sample Size	Life Cycle Stages	Class	Reference Area	T [a]	GWP [kg CO_2e/m^2a]	Note
German context								
König and Cristofaro (2012)	Germany	64	A1-A5, B1-B4, B6, C1-C4	MFH	NFA	50	6–28	
König (2017)	Germany	72	A1-A3, B2, B4, C3-C4	SFH	NFA	50	8.4–16.7	
Mahler et al. (2019)	Germany	400	A1-A3, B4, C3-C4	SFH, MFH	NFA	50	10–16	
Özdemir et al. (2022)	Germany	8	A1–A3, B2, B4, B6, C3-C4	SFH, MFH	GFA	50	12–18	
Meier-Dotzler (2023)	Germany	181	A1-A3, B4, C3-C4	MFH	NFA	50	2.1–8.0	
DGNB and BPIE (2025)	Germany	28	A1-A3, B4, C3-C4	MFH	NFA	50	10	Reference value
This study (2026)	**Germany**	**19.42 Mio.**	**A1-A3, B4, C3-C4**	**SFH, TH, MFH, AB**	**NFA**	**50**	**1.7–48.7**	**Median 7.19**
Non-German Context								
Chastas et al. (2018)	Global	95	A, B, C	n.s.[c]	n.s.	50	3.6–21	Meta-study
Lausselet et al. (2019)	Norway	695	A1-A3, B4, B6	AB, TH	NHFA	60	11	
Rasmussen et al. (2019)	Denmark	7	A1-A3, B6, C3-C4	TH, MFH	GFA	50	7.9	
Rasmussen et al. (2019)	Italy	28	A1-A5, B4, B6-B7, C2-C4	SFH, MFH	GHFA	50	5.4	
Röck et al. (2020)	Global	186	A1-A3, B6	n.s.	GFA	50	6.7–11.2	Meta-study
Schmidt et al. (2020)	Australia	n.s.	n.s.	SFH	n.s.	n.s.	8.6–11.5	
One Click LCA Ltd (2021)	Europe	1,232	A1-A4, B4-B5, C1-C4	TH, AB	n.s.	n.s.	9.2–13.8[a]	460–690 kg CO_2e/m^2
Trigaux et al. (2021)	Global	n.s.	A, B, C, D	n.s.	GFA	50	2–13	Meta-study
Heisel et al. (2022)	USA	11,049	A1-A3	n.s.	n.s.	n.s.	3.0–39.3	
Rasmussen et al. (2022)	Global	72	varies	n.s.	n.s.	n.s.	2–9	Meta-study
Röck et al. (2022)	5 EU[b]	634	A1-A5, B1-B4, C1-C4	SFH, TH, MFH	GFA	50	8–16	
Hu (2023)	USA	≫1 Mio.	A1-A5, B1-B6	SFH, TH, MFH	n.s.	60	20–144	National stock
Izaola et al. (2023)	Spain	1	A, B, C	MFH	UFA	50	11.2[a]	559 kg CO_2e/m^2
Ghorbany and Hu (2024)	USA	1 Mio.	A1-A5, B1-B7, C1-C4, D	n.s.	n.s.	50	2.5–19	
Jungclaus et al. (2024)	USA	64	A1-A3	SFH	n.s.	n.s.	0.8–2.42[a]	39–121 kg CO_2e/m^2
Szalay (2024)	Hungary	n.s.	A1-A5, B3-B4, C1-C4	SFH, MFH	NHFA	50	9.1–15.5	
Elkhayat et al. (2025)	Ireland	10	A1-A5, B4, C1-C4	SFH	UFA	50	13.2[a]	662 kg CO_2e/m^2
Gillott et al. (2025)	UK	6	A1-A3	MFH	n.s.	n.s.	5.8[a]	290 kg CO_2e/m^2
Železná et al. (2026)	Czech Republic	40	A1-A3, C3-C4	SFH, MFH	GFA	50	11.7–16.1	

[a] If accumulated embodied carbon intensity is given, we use the reference study period to calculate per annum intensity; otherwise, we consider 50 years.
[b] Belgium, Denmark, Finland, France, Netherlands.
[c] n.s. = not specified

References

Asam, C., 2017. Dämmmaßnahmen an Gebäudefassaden. Technical Report. Bundesinstitut für Bau-, Stadt- und Raumforschung (BBSR). Bonn. URL: https://www.bbsr.bund.de/BBSR/DE/veroeffentlichungen/analysen-kompakt/2017/ak-11-2017-dl.pdf.

Baunetz Wissen, 2024. Dachneigung. URL: https://www.baunetzwissen.de/glossar/d/dachneigung-48993.

BBSR, 2017. Nutzungsdauern von Bauteilen für Lebenszyklusanalysen nach Bewertungssystem Nachhaltiges Bauen (BNB). Technical Report. Bundesinstitut für Bau-, Stadt- und Raumforschung (BBSR). Bonn. URL: https://www.nachhaltigesbauen.de/fileadmin/pdf/Nutzungsdauer_Bauteile/BNB_Nutzungsdauern_von_Bauteilen_2017-02-24.pdf.

Bergner, H., Volz, H., 2012. 4 C Tragwerksentwurf und Vorbemessung, in: Schneider, K.J., Goris, A., Albert, A. (Eds.), Bautabellen für Ingenieure. Mit Berechnungshinweisen und Beispielen. 20 ed.. Werner, Köln.

Binderholz Bausysteme GmbH, n.d. Binderholz Brettsperrholz BBS. URL: https://www.binderholz.com/fileadmin/user_upload/books/de/bbs/index.html.

BMWi, BMI, 2020. Bekanntmachung der Regeln zur Datenaufnahme und Datenverwendung im Wohngebäudebestand. Technical Report. Bundesministerium für Wirtschaft und Energie (BMWi) and Bundesministerium des Innern, für Bau und Heimat (BMI). Berlin. URL: https://www.bundesanzeiger.de/pub/publication/qzQUGd8A3unSCCbVMcf?0.

BMWSB, 2020. ÖKOBAUDAT, Version 2020-II. URL: https://www.oekobaudat.de/service/downloads.html. Accessed 2021-04-06.

Chastas, P., Theodosiou, T., Kontoleon, K.J., Bikas, D., 2018. Normalising and assessing carbon emissions in the building sector: A review on the embodied CO2 emissions of residential buildings. Building and Environment 130, 212–226. doi:10.1016/j.buildenv.2017.12.032.

Cischinsky, H., Diefenbach, N., 2016. Datenerhebung Wohngebäudebestand 2016. Datenerhebung zu den energetischen Merkmalen und Modernisierungsraten im deutschen und hessischen Wohngebäudebestand. Technical Report. Institut für Wohnen und Umwelt (IWU). URL: https://wohngebaeudedaten2016.iwu.de/dl/Endbericht%20Datenerhebung%20WohngebÃ‌udebestand%202016.pdf.

Colling, F., 2012. Holzbau nach Eurocode 5, in: Schneider, K.J., Goris, A., Albert, A. (Eds.), Bautabellen für Ingenieure. Mit Berechnungshinweisen und Beispielen. 20 ed.. Werner, Köln.

Dabrock, K., Pflugradt, N., Weinand, J.M., Stolten, D., 2024a. Leveraging machine learning to generate a unified and complete building height dataset for Germany. Energy and AI 17, 100408. doi:10.1016/j.egyai.2024.100408.

Dabrock, K., Ulken, J., Pflugradt, N., Weinand, J.M., Stolten, D., 2024b. ETHOS.BUILDA: Residential building TABULA archetype dataset Germany. doi:10.5281/zenodo.13771740.

Dabrock, K., Ulken, J., Pflugradt, N., Weinand, J.M., Stolten, D., 2025. Generating a nationwide residential building types dataset using machine learning. Building and Environment 274, 112782. doi:10.1016/j.buildenv.2025.112782.

dataholz.eu, 2021. Katalog bauphysikalisch und ökologisch geprüfter Holzbauteile. URL: https://www.dataholz.eu/index.html.

Destatis, 2003–2020. Bautätigkeit und Wohnungen. Bautätigkeit (Fachserie 5, Reihe 1). Technical Report. Statistisches Bundesamt (Destatis). Wiesbaden. URL: https://www.statistischebibliothek.de/mir/receive/DESerie_mods_00000075.

DGNB, BPIE, 2025. Lebenszyklusbasierte betrachtung von gebäuden: Eine analyse von 28 wohngebäuden zu klimawirkungen und kosten. URL: https://www.dgnb.de/de/nachhaltiges-bauen/klimaschutz/toolbox/publikationen-zum-klimaschutz. accessed 15.05.2026.

DIN Deutsches Institut für Normung e. V., 2010. DIN EN ISO 10456:2010-05: Baustoffe und Bauprodukte - Wärme- und feuchtetechnische Eigenschaften - Tabellierte Bemessungswerte. Norm.

DIN Deutsches Institut für Normung e. V., 2012. DIN EN 15978:2012-10: Sustainability of construction works - Assessment of environmental performance of buildings - Calculation method. Norm. doi:10.31030/1917049.

DIN Deutsches Institut für Normung e. V., 2017a. DIN 18531-1:2017-07: Abdichtung von Dächern sowie von Balkonen, Loggien und Laubengängen - Teil 1. Norm.

DIN Deutsches Institut für Normung e. V., 2017b. DIN 18531-3:2017-07: Abdichtung von Dächern sowie von Balkonen, Loggien und Laubengängen - Teil 3. Norm.

DIN Deutsches Institut für Normung e. V., 2017c. DIN 18533-1:2017-07: Abdichtung von erdberührten Bauteilen - Teil 1. Norm.

DIN Deutsches Institut für Normung e. V., 2017d. DIN 18533-3:2017-07: Abdichtung von erdberührten Bauteilen - Teil 3. Norm.

DIN Deutsches Institut für Normung e. V., 2018. DIN 276:2018-12: Kosten im Bauwesen. Norm.

DIN Deutsches Institut für Normung e. V., 2020a. DIN 4108-4:2020-11: Wärmeschutz und Energie-Einsparung in Gebäuden - teil 4: Wärme- und feuchteschutztechnische Bemessungswerte. Norm.

DIN Deutsches Institut für Normung e. V., 2020b. DIN EN ISO 10077-1:2020-10: Wärmetechnisches Verhalten von Fenstern, Türen und Abschlüssen - Berechnung des Wärmedurchgangskoeffizienten - Teil 1: Allgemeines. Norm.

DIN Deutsches Institut für Normung e. V., 2021. DIN 277:2021-08: Grundflächen und Rauminhalte im Hochbau. Norm.

DIN Deutsches Institut für Normung e. V., 2022. DIN EN 15804:2022-03: Sustainability of construction works - Environmental product declarations - Core rules for the product category of construction products. Norm. URL: https://www.dinmedia.de/de/norm/din-en-15804/344735627.

Eicke-Hennig, W., 2017. Vom Flechtwerk zum Dämmpaket. Historischer Wärmeschutz: Geschichte der Dämmstoffe. Technical Report. Energieinstitut Hessen. Frankfurt am Main. URL: https://www.nei-dt.de/Downloads/Geschichte%20der%20Daemmstoffe-Eicke-Hennig-2017.pdf.

Elkhayat, Y., Moran, P., McElmeel, H., 2025. Evaluating, benchmarking, and reducing embodied carbon of deep retrofit homes with significant extension: Irish case studies. Cleaner Environmental Systems 18, 100317. doi:10.1016/j.cesys.2025.100317.

Figl, H., Brockmann, T., Huemer-Kals, V., Kusche, O., Kerz, N., Rössig, S., 2019. Ökobaudat. Grundlage für die Gebäudeökobilanzierung. Technical Report. Bundesinstitut für Bau-, Stadt- und Raumforschung (BBSR). Bonn. URL: https://www.oekobaudat.de/fileadmin/downloads/0068G_BF_200106ms.pdf.

Fischer, O., Winter, S., Lang, W., Dotzler, C., Hessinger, J., Kurzer, C., Schneider-Marin, P., Volz, C., 2019. Hybridbau: Holzaußenwände. DETAIL Praxis, DETAIL, München.

Ghorbany, S., Hu, M., 2024. Urban embodied carbon assessment: methodology and insights from analyzing over a million buildings in Chicago. Carbon Management 15, 2382993. doi:10.1080/17583004.2024.2382993.

Giebeler, G., Fisch, R., Krause, H., Musso, F., Petzinka, K.H., Rudolphi, A., 2008. Atlas Sanierung. Instandhaltung, Umbau, Ergänzung. Birkhäuser, München. doi:doi:10.11129/detail.9783034614344.

Gillott, C., Lanau, M., Mitchell Reid, E., Sharmin, F., Densley Tingley, D., 2025. Material stocks and embodied carbon in UK buildings: An archetype-based, bottom-up, GIS approach. Journal of Industrial Ecology 29, 1748–1762. doi:10.1111/jiec.70066.

Goris, A., Schmitz, U., 2012. Stahlbeton- und Spannbetonbau nach Eurocode 2, in: Schneider, K.J., Goris, A., Albert, A. (Eds.), Bautabellen für Ingenieure. Mit Berechnungshinweisen und Beispielen. 20 ed.. Werner, Köln.

Gruhler, K., Böhm, R., Deilmann, C., Schiller, G., 2002. Stofflich-energetische Gebäudesteckbriefe - Gebäudevergleiche und Hochrechnungen für Bebauungsstrukturen. volume 38 of *IÖR Schriften*. Leibniz-Institut für ökologische Raumentwicklung e.V. (IÖR), Dresden.

Hauser, G., Lüking, M., Verband Fenster + Fassade (VFF), Bundesverband Flachglas (BF), 2017. Mehr Energie sparen mit neuen Fenstern. Technical Report. Verband Fenster + Fassade and Bundesverband Flachglas. Frankfurt am Main. URL: https://www.window.de/wp-content/uploads/fileadmin/redaktion_window/vff/docs_und_pdf/VFF-BF_Studie_Mehr_Energie_sparen_mit_neuen_Fenstern_2017-09.pdf.

Heisel, F., McGranahan, J., Ferdinando, J., Dogan, T., 2022. High-resolution combined building stock and building energy modeling to evaluate whole-life carbon emissions and saving potentials at the building and urban scale. Resources, Conservation and Recycling 177, 106000. doi:10.1016/j.resconrec.2021.106000.

Hu, M., 2023. A look at residential building stock in the United States - mapping life cycle embodied carbon emissions and other environmental impact. Sustainable Cities and Society 89, 104333. doi:10.1016/j.scs.2022.104333.

Höglmeier, K., Weber-Blaschke, G., Richter, K., 2013. Potentials for cascading of recovered wood from building deconstruction—a case study for south-east germany. Resources, Conservation and Recycling 78, 81–91. doi:https://doi.org/10.1016/j.resconrec.2013.07.004.

InformationsZentrum Beton, 2019. Zement-Merkblatt Hochbau H 10: Wasserundurchlässige Bauwerke aus Beton. Technical Report. InformationsZentrum Beton GmbH. URL: https://www.vdz-online.de/wissensportal/publikationen/zement-merkblatt-h10-wasserundurchlaessige-bauwerke-aus-beton.

Izaola, B., Akizu-Gardoki, O., Oregi, X., 2023. Setting baselines of the embodied, operational and whole life carbon emissions of the average Spanish residential building. Sustainable Production and Consumption 40, 252–264. doi:10.1016/j.spc.2023.07.001.

IÖR, n.d. Bauwerksdaten. Wohngebäude. URL: http://ioer-bdat.de/bauwerksdaten/wohngebaeude/.

Jungclaus, M.A., Grant, N., Torres, M.I., Arehart, J.H., Srubar, W.V., 2024. Embodied carbon benchmarks of single-family residential buildings in the United States. Sustainable Cities and Society 117, 105975. doi:10.1016/j.scs.2024.105975.

KS-Original GmbH, 2021. Produkte. URL: https://www.ks-original.de/produkte.

König, H., 2017. Lebenszyklusanalyse mit Berechnung der Ökobilanz und Lebenszykluskosten. Technical Report. Bayerisches Landesamt für Umwelt. URL: https://www.biv.bayern/biv.bayern/media/bauen/endbericht-lebenszyklusanalyse-von-wohngebaeuden.pdf. accessed 31.03.2026.

König, H., Cristofaro, M.L.D., 2012. Benchmarks for life cycle costs and life cycle assessment of residential buildings. Building Research & Information 40, 558–580. doi:10.1080/09613218.2012.702017.

Lausselet, C., Borgnes, V., Brattebø, H., 2019. LCA modelling for Zero Emission Neighbourhoods in early stage planning. Building and Environment 149, 379–389. doi:10.1016/j.buildenv.2018.12.034.

Loga, T., Diefenbach, N., Stein, B., Born, R., 2012. TABULA - scientific report Germany; further development of the national residential building typology. URL: https://www.episcope.eu/downloads/public/docs/scientific/DE_TABULA_ScientificReport_IWU.pdf.

Loga, T., Stein, B., Diefenbach, N., 2016. TABULA building typologies in 20 European countries—making energy-related features of residential building stocks comparable. Energy and Buildings 132, 4–12. doi:10.1016/j.enbuild.2016.06.094.

Mahler, B., Idler, S., Nusser, T., Gantner, J., 2019. Energieaufwand für Gebäudekonzepte im gesamten Lebenszyklus. Technical Report UFOPLAN FKZ 3715 41 111 0. Umweltbundesamt. URL: https://www.bundesumweltministerium.de/fileadmin/Daten_BMU/Pools/Forschungsdatenbank/fkz_3715_41_111_energieaufwand_gebaeudekonzepte_bf.pdf. accessed 31.03.2026.

Meier-Dotzler, C.M., 2023. Lebenszyklusbasierte ökologische Kennwertentwicklung von Gebäudekonstruktionen im Alt- und Neubau zur Anwendung in 3D-Stadtmodellen. Ph.D. thesis. Technische Universität München. URL: https://mediatum.ub.tum.de/1695838.

Metzger, S., Jahnke, K., Walikewitz, N., Otto, M., Grondey, A., Fritz, S., 2019. Wohnen und Sanieren - Empirische Wohngebäudedaten seit 2002. Technical Report CLIMATE CHANGE 22/2019. Umweltbundesamt. Dessau-Roßlau. URL: https://www.umweltbundesamt.de/system/files/medien/1410/publikationen/2019-05-23_cc_22-2019_wohnenundsanieren_hintergrundbericht.pdf. accessed 01.04.2026.

One Click LCA Ltd, 2021. Embodied carbon benchmarks for European buildings. URL: https://oneclicklca.com/hubfs/Ebooks/Embodied-Carbon-Benchmarks-for-European-Buildings-10-June-2021-FINAL.pdf. accessed 31.03.2026.

Optigrün international AG, 2021. Dachbegrünung Spardach. Der beliebte Optigrün-Standardaufbau für extensive Dachbegrünungen. URL: https://www.optigruen.de/systemloesungen/spardach.

Passive House Institute, 2023. Criteria for Buildings. Technical Report. Passive House Institute. Darmstadt. URL: https://univention.passiv.de/nextcloud/s/version10c-2023-ip?dir=/&editing=false&openfile=true.

Pomponi, F., Moncaster, A., 2018. Scrutinising embodied carbon in buildings: The next performance gap made manifest. Renewable and Sustainable Energy Reviews 81, 2431–2442. doi:10.1016/j.rser.2017.06.049.

Qin, Y., Suh, S., 2017. What distribution function do life cycle inventories follow? The International Journal of Life Cycle Assessment 22, 1138–1145. doi:10.1007/s11367-016-1224-4.

Rasmussen, F.N., Ganassali, S., Zimmermann, R.K., Lavagna, M., Campioli, A., Birgisdóttir, H., 2019. LCA benchmarks for residential buildings in Northern Italy and Denmark – learnings from

comparing two different contexts. Building Research & Information 47, 833–849. doi:10.1080/09613218.2019.1613883.

Rasmussen, F.N., Trigaux, D., Alsema, E., Balouktsi, M., Birgisdóttir, H., Bohne, R., Dixit, M., Dowdell, D., Francart, N., Frischknecht, R., Foliente, G., Lupisek, A., Lützkendorf, T., Malmqvist, T., Garcia Martinez, A., Ouellet-Plamondon, C., Passer, A., Peuportier, B., Ramseier, L., Satola, D., Seo, S., Szalay, Z., Wiik, M., 2022. Existing benchmark systems for assessing global warming potential of buildings – analysis of IEA EBC Annex 72 cases. IOP Conference Series: Earth and Environmental Science 1078, 012054. doi:10.1088/1755-1315/1078/1/012054.

Röck, M., Saade, M.R.M., Balouktsi, M., Rasmussen, F.N., Birgisdottir, H., Frischknecht, R., Habert, G., Lützkendorf, T., Passer, A., 2020. Embodied GHG emissions of buildings – the hidden challenge for effective climate change mitigation. Applied Energy 258, 114107. doi:10.1016/j.apenergy.2019.114107.

Röck, M., Sørensen, A., Tozan, B., Steinmann, J., Horup, L.H., Le Den, X., Birgisdottir, H., 2022. Towards embodied carbon benchmarks for buildings in Europe - #2 setting the baseline: A bottom-up approach. doi:10.5281/zenodo.5895051.

Schlemminger, M., Bredemeier, D., Mahner, A., Niepelt, R., Breitner, M.H., Brendel, R., 2024. Rooftop PV potential determined by backward ray tracing: A case study for the German regions of Berlin, Cologne, and Hanover. Progress in Photovoltaics: Research and Applications 32, 912–929. doi:10.1002/pip.3844.

Schmidt, M., Crawford, R.H., Warren-Myers, G., 2020. Quantifying Australia's life cycle greenhouse gas emissions for new homes. Energy and Buildings 224, 110287. doi:10.1016/j.enbuild.2020.110287.

Schneider-Marin, P., Dotzler, C., Röger, C., Lang, W., Glöggler, J., Meier, K., Runkel, S., 2019. Design2Eco. Lebenszyklusbetrachtung im Planungsprozess von Büro- und Verwaltungsgebäuden. Technical Report. Forschungsinitiative Zukunft Bau, Bundesinstitut für Bau-, Stadt- und Raumforschung (BBSR). Stuttgart. URL: https://www.irbnet.de/daten/rswb/19039016001.pdf.

Sprengard, C., Treml, S., Holm, A.H., 2014. Technologien und Techniken zur Verbesserung der Energieeffizienz von Gebäuden durch Wärmedämmstoffe Metastudie. Wärmedämmstoffe - Produkte - Anwendungen - Innovationen. Technical Report. Forschungsinstitut für Wärmeschutz e.V. München (FIW). Stuttgart. URL: https://www.irbnet.de/daten/Inhaltsverzeichnisse/fb_F_2909.pdf.

Szalay, Z., 2024. A parametric approach for developing embodied environmental benchmark values for buildings. The International Journal of Life Cycle Assessment 29, 1563–1581. doi:10.1007/s11367-024-02322-w.

Thamling, N., Rau, D., Kemmler, A., Sahnoun, M., Kulkarni, P., Vu, M.P., 2022. Hintergrundpapier zur Gebäudestrategie Klimaneutralität 2045. Technical Report. Prognos AG, Gutachten im Auftrag des Bundesministeriums für Wirtschaft und Klimaschutz. Berlin. URL: https://www.bundeswirtschaftsministerium.de/Redaktion/DE/Publikationen/Klimaschutz/gebaeudestrategie-klimaneutralitaet-2045.html.

Thiel, D., Riedel, D., 2011. Typisierte Bauteilaufbauten - Präzisierung der Pauschalwerte für Wärmedurchgangskoeffizienten aus der Bekanntmachung der Regeln der Datenaufnahme im Nichtwohngebäudebestand. Technical Report. Forschungsinitiative Zukunft Bau, Bundesinstitut für Bau-, Stadt- und Raumforschung (BBSR). Stuttgart. URL: https://www.irbnet.de/daten/rswb/11109001108.pdf.

Trigaux, D., Allacker, K., Debacker, W., 2021. Environmental benchmarks for buildings: a critical literature review. The International Journal of Life Cycle Assessment 26, 1–21. doi:10.1007/s11367-020-01840-7.

Verband Fenster + Fassade (VFF), Bundesverband Flachglas (BF), n.d. Produktentwicklung und Produktdatenblätter: Fenster und Glas im Bestand. Technical Report. Verband Fenster + Fassade and Bundesverband Flachglas. URL: https://www.window.de/wp-content/uploads/fileadmin/redaktion_window/vff/Normung_und_Technik_pdfs/Fenster_im_Bestand_Grafik.pdf. accessed 2020-04-16.

Wienerberger GmbH, 2021. Produktkatalog Porotonziegel. URL: https://www.wienerberger.de/produkte/wand/ziegel.html?loadmore=2.

Woytowicz, J., Stöckle, L., Präger, L., Lang, W., 2025. Determination of a dynamic top-down greenhouse gas budget for buildings in Germany. IOP Conference Series: Earth and Environmental Science 1554, 012121. doi:10.1088/1755-1315/1554/1/012121.

Xella Deutschland GmbH, n.d. Das Baubuch. Sicher planen und bauen. Technical Report. Xella Deutschland GmbH. URL: https://technik.xella.de/media/books/baubuch/428/. 5th edition. Accessed 2021-10-01.

Zentrum für Umweltbewusstes Bauen, 2009. Erfassung regionaltypischer Materialien im Gebäudebestand mit Bezug auf die Baualtersklasse und Ableitung typischer Bauteilaufbauten. Technical Report. Zentrum für Umweltbewusstes Bauen e.V.. Kassel. URL: https://www.nei-dt.de/Downloads/ZUB-Erfassung%20regionaltypischer%20Materialien%20im%20Gebaeudebestand.pdf.

Özdemir, Ö., Hartmann, C., Hafner, A., König, H., Lützkendorf, T., 2022. Next generation of life cycle related benchmarks for low carbon residential buildings in Germany. IOP Conference Series: Earth and Environmental Science 1078, 012053. doi:10.1088/1755-1315/1078/1/012053.

Überwachungsgemeinschaft Konstruktionsvollholz e.V., 2020. Konstruktionsvollholz KVH und Balkenschichtholz (Duobalken, Triobalken). volume Reihe 4, Teil 2, Folge 1 of *Holzbau Handbuch*. 5 ed., Überwachungsgemeinschaft Konstruktionsvollholz e.V., Wuppertal. URL: https://informationsdienst-holz.de/fileadmin/Publikationen/2_Holzbau_Handbuch/R04_T02_F01_Konstruktionsvollholz_KVH-und-Balkenschichtholz--Duobalken-Triobalken_2020-03.pdf.

Železná, J., Felicioni, L., Růžička, J., Diviš, J., Fořtová, K., Nehasilová, M., Trubina, N., Vlasatá, B., Veselka, J., 2026. Whole life carbon assessment of Czech building typologies: analysis of 170 representative case studies towards the definition of national benchmarks. Building and Environment 297, 114556. doi:10.1016/j.buildenv.2026.114556.